The C-Fe (Carbon-Iron) System

by H. Okamoto
ASM International

Equilibrium Diagram

The number of experimental and theoretical publications on the Fe-C phase diagrams and related subjects is *virtually unlimited* because of the unquestionable importance of Fe-C alloys in all aspects of human activities. The details of the stable and metastable phase diagrams of the Fe-C system, especially on the Fe-rich side, are known much better than any other binary systems with similar complexity. However, there are still substantial areas where the phase diagram has not been well established—in the temperature, composition, and pressure ranges not related directly to iron and steel making.

In the present evaluation, the assessed stable Fe-C (graphite) and metastable Fe-Fe_3C (cementite) equilibrium phase diagrams for 0 to 25 at.% C are based on thermodynamic calculations reported by [79Sch1] and [84Oht]. Comparison of these calculated results with experimental data indicates that the uncertainty of the diagrams is approximately ± 2 °C and ± 0.1 at.%. The phase diagrams in the remaining composition range and at pressures other than 1 atm are less certain. One of the reasons for this uncertainty is that even the transition temperatures of pure Fe are not well determined. Although the reference temperature scale varied among quoted reports, the experimental data are cited in this evaluation as given in the original papers; attempts to correct temperatures would have been meaningless in *many instances* due to more grave problems, such as unknown impurities in alloys, cooling/heating rate effect, and uncertainty in the chemical composition of specimens.

The stable equilibrium phases of the Fe-C system at ambient pressure are (1) the gas, g; (2) the liquid, L; (3) bcc (δFe); (4) fcc (γFe), or austenite; (5) bcc (αFe), or ferrite; and (6) hexagonal (C), or graphite. Orthorhombic Fe_3C, or cementite, is a metastable phase. However, the metastable Fe-Fe_3C system is discussed in this section together with the stable Fe-C system. The alphabetical designations at special points in the phase diagrams are adopted from [Hansen] for *A* to *S* except for *I* and *R*, and from [79Sch2] for *R* to *W* except for *S*. Figure 1 shows a conventional Fe-C and Fe-Fe_3C double diagram, and Table 1 summarizes the reaction types and coordinates of special points.

Experimental Methods

The experimental methods used to determine the phase boundaries are not cited here in complete detail because the sources are numerous. The primary methods used are thermal analysis [1897Rob, 1899Rob, 00Bak, 04Car, 04Hey, 12Meu, 13Hon, 14Rue, 14Ruf, 14Rum, 16Bar, 20Rue, 21Mau, 21Rue, 26Ell, 29And, 30Har, 34Piw, 37Adc, 38Wel, 60Buc, 64Ver, 82Chi, 83Chi], chemical analysis of equilibrated samples [07Cha, 09Gut, 11Han, 11Rue, 11Ruf, 12Wit, 14Ruf, 29Sch, 31Soh, 42Gur, 49Sta, 52Chi, 52Kit, 55Lin, 55Mat, 55Tur, 59Smi1, 61Ben, 61Sch1, 61Sch2, 62Smi, 63Mor, 64Cah, 66Nak, 71Wad, 85Has], metallography [1897Rob, 1899Rob, 09Gut, 10Goe, 11War, 14Sal, 17Tsc, 37Meh], composition dependence of physical properties such as magnetism and thermodynamic activities [49Dij, 51Dar, 52Fal, 58Gen, 58Pet, 59Heu, 59Sin, 60Sin, 67Swa, 69Swa, 70Ban], temperature dependence of physical

Table 1 Special Points of the Assessed Fe-C Phase Diagram

Reaction	Composition of the respective phases, at.% C			Temperature, °C	Reaction type
Stable Fe-C (graphite) system					
g ↔ L		0		2862	Boiling
L ↔ δFe		0		1536	Melting
δFe ↔ γFe		0		1392	Allotropic
γFe ↔ αFe		0		911	Allotropic
L + (δFe) ↔ (γFe)	2.43	0.40	0.74	1493	Peritectic
(γFe) ↔ (αFe) + (C)	2.97	0.096	100	740	Eutectoid
L ↔ (γFe) + (C)	17.1	9.06	100	1153	Eutectic
g ↔ C (graphite)		100		3826	Sublimation
Metastable Fe-Fe_3C (cementite) system					
(γFe) ↔ (αFe) + Fe_3C	3.46	0.104	25	727	Eutectoid
L ↔ (γFe) + Fe_3C	17.3	9.23	25	1147	Eutectic
L ↔ Fe_3C		25		1252	Congruent

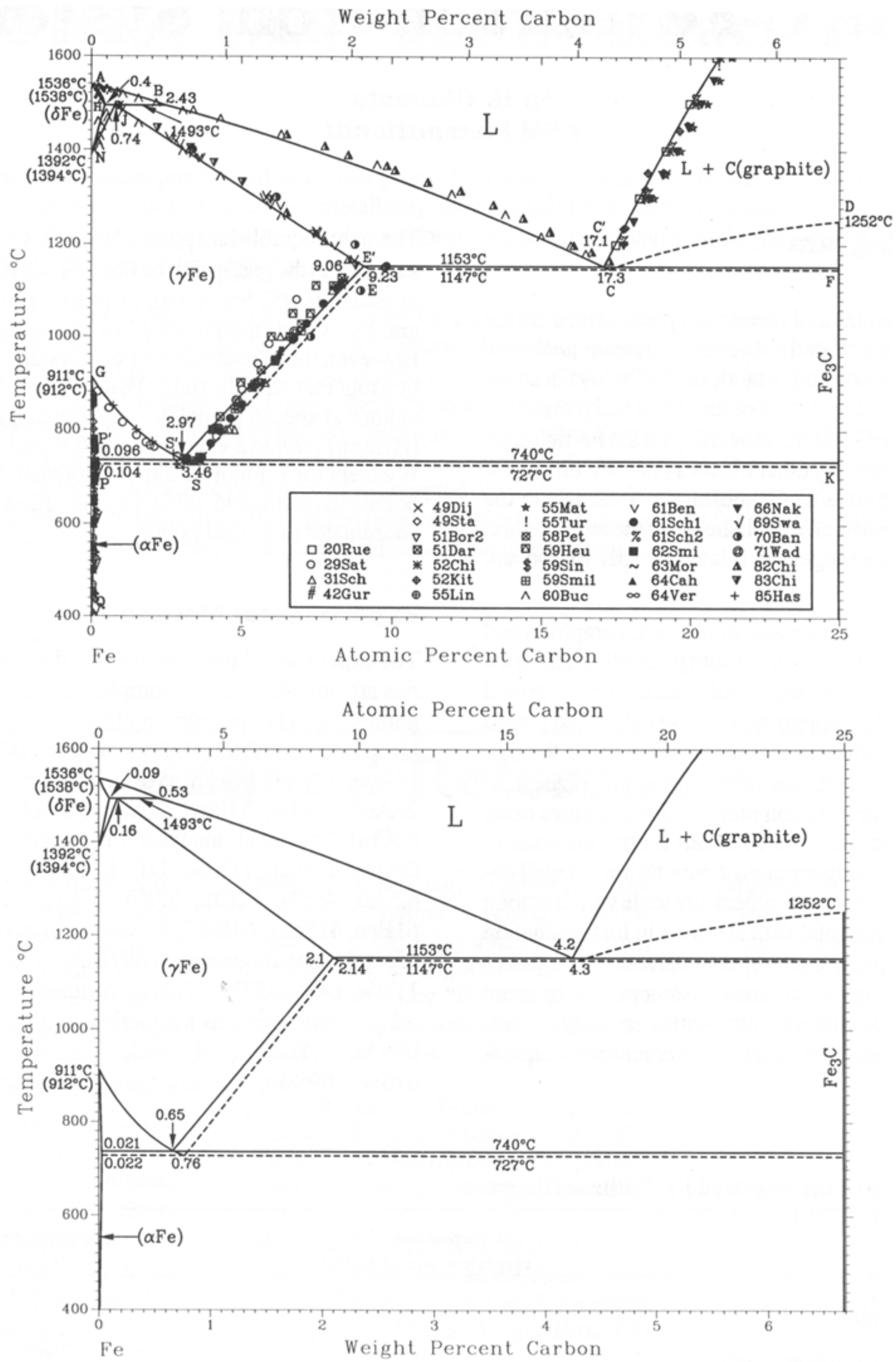

Fig. 1 Assessed Fe-C phase diagram from 0 to 25 at.% Fe. Stable Fe-C (graphite) and metastable Fe-Fe_3C (cementite) equilibria. Temperatures in parentheses are recommended by [Massalski2].

properties such as electrical resistance and magnetism [13Hon, 15Sal, 16Hon, 18Iit, 23Asa, 23Ber, 23Kon, 25Kay, 26Sta, 27Ess, 27Hon1, 27Hon2, 27Hon3, 29Sat, 37Meh, 50Wer, 67Fil], and kinetics of precipitation [51Bor1, 51Bor2]. Because of the overwhelming number of data points, only selected points are shown in the assessed diagram.

Review

Toward the end of the 19th century, [1899Rob] and [00Bak] proposed the first phase diagram representations of the Fe-C system. Although their diagrams are crude by present standards (for example, the (δFe) phase was unknown), the key features of the

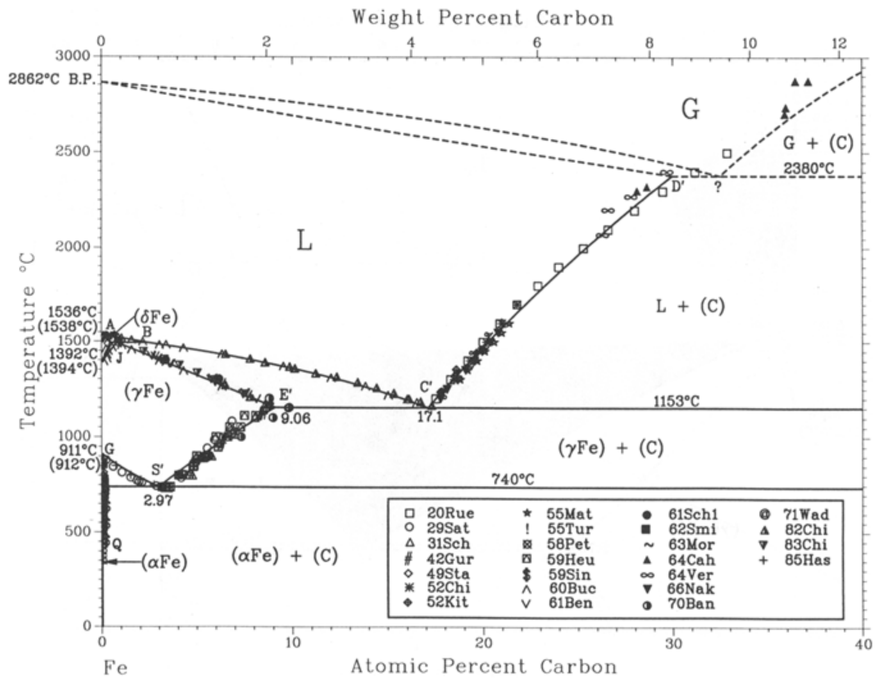

Fig. 2 Assessed Fe-C (graphite) phase diagram. Temperatures in parentheses are recommended by [Massalski2].

Table 2 Calculated Fe-C Special Points

	[79Sch1]		[84Oht]		[85Gus]	
Point	Temperature, °C	Composition, at.% C	Temperature, °C	Composition, at.% C	Temperature, °C	Composition, at.% C
H	1493	0.40	1494	0.38	1495	0.42
J	1493	0.74	1494	0.79	1495	0.83
B	1493	2.43	1494	2.30	1495	2.41
E′	1153	9.06	1154	8.95	1154	9.36
C′	1153	17.13	1154	17.28	1154	19.87
E	1147	9.23	1147	9.03	1148	9.46
C	1147	17.29	1147	17.45	1148	20.04
P′	736	0.15	740	0.096	738	0.083
S′	736	3.12	740	2.97	738	3.09
P	727	0.16	727	0.104	727	0.088
S	727	3.43	727	3.46	727	3.44

double equilibria for the Fe-C and Fe-Fe_3C systems were discovered by these investigators. All aspects of the Fe-C diagrams shown in Fig. 1 had been revealed when [32Goe] reviewed this system. Later, the positions of phase boundaries were refined by numerous experimental reports, as mentioned above. Thermodynamic approaches to represent the phase diagrams by [50Wer], [53Dar], [54Hil], [55Hil], [61Ben], [68Wad], [71Har], [72Chi], [74Bas], [78Sch], [79Agr], [79Sch1], [84Oht], and [85Gus] clarified several uncertain features that experiments had failed to define.

Earlier literature on the Fe-C system was listed in a review article by [36Eps]. [Hansen] covered information published prior to 1955. A review in [Metals], with the Fe-C phase diagram based primarily on [72Chi], has been serving as one of the standard Fe-C phase diagrams until now. However, [79Agr] and [84Oht] pointed out errors in the thermodynamic model of [72Chi]. [82Kub] accepted phase diagrams derived thermodynamically by [79Sch1] and [79Sch2]. A more recent review by [86Ban] was based on relatively old information.

Transformation Temperatures of Fe

The boiling point temperature of Fe is 2862 °C [Massalski2].

According to IPTS-68 [Melt], the melting point of δFe is 1535 °C (secondary reference point), whereas [82Swa] recommended 1538 °C. The melting point accepted in this evaluation is 1536 °C [Hultgren, E], which was adopted in thermodynamic models by

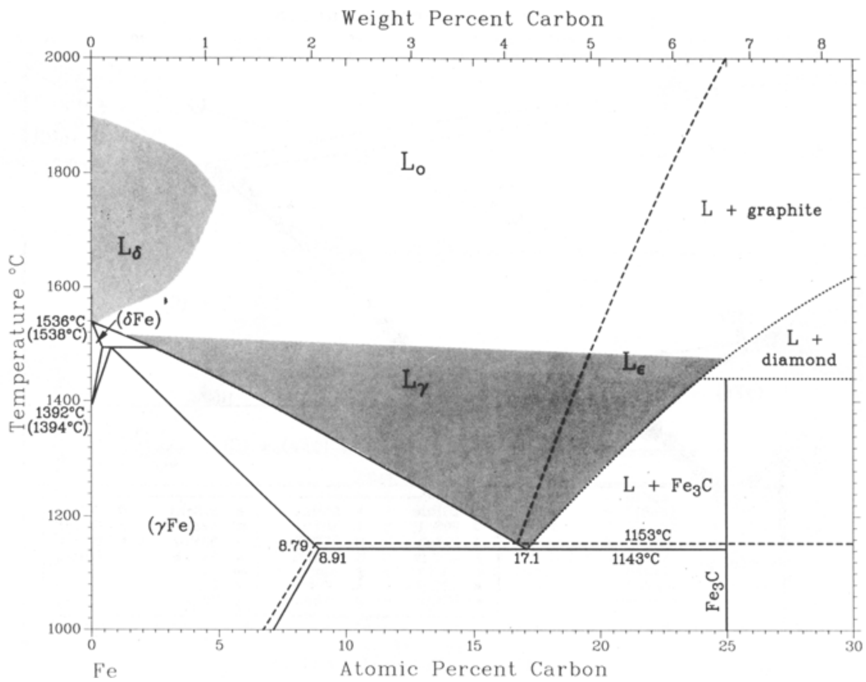

Fig. 3 Regions of short-range order in the Fe-C liquid phase. From [69Gri]. Temperatures in parentheses are recommended by [Massalski2].

[79Sch1] and [84Oht]. Because of the large uncertainty (± 5 °C) in the data on which both IPTS-68 and [82Swa] were based, adjustment of the melting point of Fe is not feasible at this time.

Similarly, the δFe ↔ γFe and γFe ↔ αFe allotropic transformation temperatures are accepted from [Hultgren, E] as 1392 and 911 °C, respectively. [82Swa] recommended 1394 and 912 °C, respectively.

Stable Fe-C (Graphite) System

The assessed phase boundaries among condensed phases in Fig. 2 were derived from the results of thermodynamic calculations by [79Sch1], [84Oht], and [85Gus]. Agreement between [79Sch1] and [84Oht] is excellent (see Table 2), and they are consistent with experimental phase boundary and thermodynamic data. In this evaluation, the values of [79Sch1] are accepted primarily because the same model was used to calculate the metastable phase boundaries in [79Sch2]. However, the results of [84Oht] are accepted for the (αFe) phase boundaries, because the ferromagnetic effects in (αFe) are considered in the thermodynamic functions, and the agreement with the experimental data is better. For other regions, the slight disagreement between [79Sch1] and [84Oht] is well within the accuracy of experimental data.

Gas Phase

The gas phase field is shown in Fig. 2. The g ↔ L + (C) transition temperature is 2380 °C [64Ver], which was determined from five thermal analysis data. Earlier, [14Ruf] had proposed an Fe-C diagram including the gas phase; however, the boiling point of Fe in [14Ruf] (~2450 °C) was too low.

Liquid Phase

Short-range ordering in liquid Fe was reported by [67Fil] and [69Gri]. The liquid phase field comprises statistically disordered L_0, bcc δFe-based L_δ, fcc γFe-based L_γ, and cph εFe-based L_ε regions. Approximate extents of these regions are shown in Fig. 3. [67Fil] observed changes in density and anomalies in electrical conductivity at the boundaries among these regions.

The liquidus *AB* calculated by [79Sch1] agrees well with that measured by [60Buc] (Fig. 4). *AB* liquidus data are available also in [29And], [37Adc], and [67Fil]. [37Adc] and [60Buc] estimated the composition of point *B* to be 2.33 and 2.47 at.% C, respectively, in good agreement with calculated values (Table 2).

The liquidus *BC′* (Fig. 2) was determined by many investigators, including [1897Rob], [1899Rob], [00Bak], [09Gut], [14Rue], [17Rue], [27Hon3], [29And], [35Umi], [37Adc], [60Buc], [64Fis], [67Fil], [69Kra], and [82Chi]. The assessed *BC′* line is taken from [79Sch1].

The L ↔ (γFe) + (C) eutectic temperature was reported as 1152 [59Heu], 1153 [17Rue, 61Ben, 61Sch1, 69Gri], 1154 to 1155 [34Piw], or 1155 °C [30Kas], all in agreement with the assessed temperature (1153 °C). The composition of the eutectic point *C′* was found to be 16.75 [17Rue], 17.1 [20Rue], or 17.3 at.% C [60Buc], whereas the calculated value is 17.13 at.% C [79Sch1].

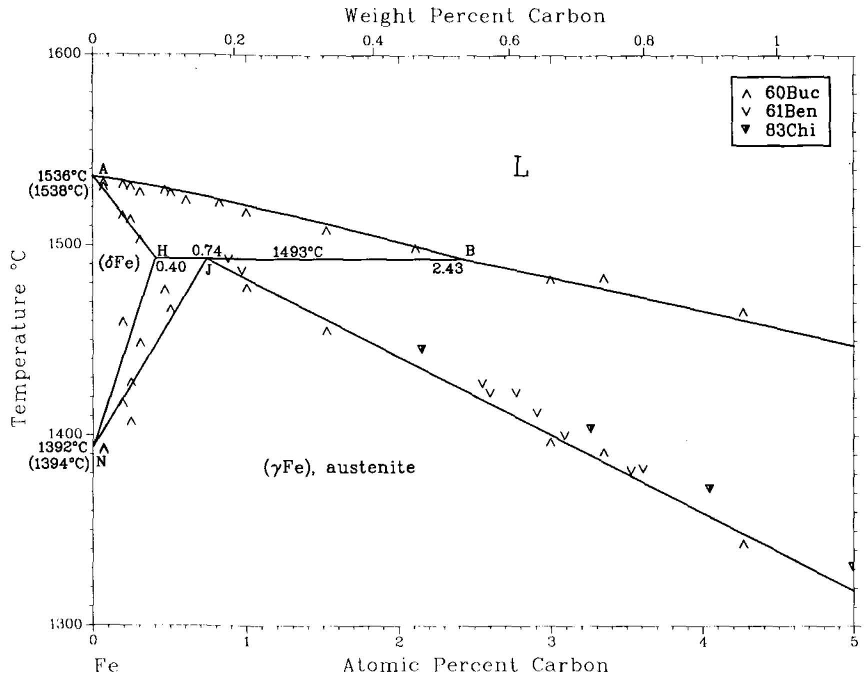

Fig. 4 (δFe) phase field of the Fe-C system. Temperatures in parentheses are recommended by [Massalski2].

The liquidus *C′D′* (Fig. 2) was measured by [11Han], [11Ruf], [12Wit], [14Ruf], [20Rue], [29Sch], [52Chi], [52Kit], [55Mat], [55Tur], [61Sch2], [63Loe], [63Mor], [64Cah], [64Ver], and [66Nak]. The assessed *C′D′* line is from [79Sch1], which agrees well with these data. Earlier, [56Tur] calculated the *C′D′* boundary up to 1500 °C using the thermodynamic data available at that time. The *C′D′* boundary data reported by [20Rue] and [64Cah] for temperatures above the g ↔ L + (C) reaction temperature (2380 °C) may be at higher pressures.

(δFe) Phase

The solidus *AH* calculated by [79Sch1] agrees with that measured by [60Buc] (Fig. 4). The solvus *NH* was measured by [14Rue], [29And], [37Adc], and [60Buc]. Because the (δFe) + (γFe) two-phase field is narrow, some data for *HN* and *JN* are not distinguishable. The line calculated by [79Sch1] is accepted in Fig. 2 (enlarged in Fig. 4). The composition of the point *H* was reported to be 0.33 [14Rue, 35Umi], 0.46 [37Adc], or 0.5 at.% C [60Buc]. The calculated value by [79Sch1] is 0.40 at.% C. Considering the uncertainty in experimental data, these values are essentially in agreement.

(γFe) Phase

The composition of point *J* was reported to be 0.60 [35Umi], 0.74 [37Adc], 0.75 [60Buc], or 0.83 at.% C [14Rue]. The value calculated by [79Sch1] is 0.74 at.% C, which is accepted in Fig. 2 (enlarged in Fig. 4) as a good representative of experimental data. Most data points for the line *NJ* are indistinguishable from those for the line *HN* (see the "(δFe) Phase" section). The line calculated by [79Sch1] is accepted in Fig. 2.

There are two distinct sets of data on the solidus *JE′*; one comprises the results of [04Car], [26Ell], [29And], [29Jom], [32Kor], [37Adc], [42Gur], [46Smi], [60Buc], [61Ben], [64Fis], [64Sch], [67Fil], [70Ban], [82Chi], and [83Chi], and the other includes those of [09Gut], [23Asa], [25Kay], [27Hon2], and [35Umi]. The agreement is surprisingly good within each group, but the temperature of the second set is ~ 100 °C lower than that of the first set at 5 at.% C (not shown in Fig. 1). [30Ell] pointed out that the second set of data does not represent equilibrium conditions. Thermodynamic calculation by [79Sch1] supports the first set of data (Fig. 2).

The L + (δFe) ↔ (γFe) peritectic temperature was observed at 1487 °C (41 °C below the assumed melting point), [14Rue, 35Umi], 1493 °C (40 °C below) [37Adc], 1493 °C (47 °C below) [64Ver, 65Ver], 1494 °C (42 °C below) [60Buc], 1495 °C (42 °C below) [29And], and 1499 °C (37 °C below) [61Ben] (the temperature may be too high by 1.5 °C due to reference to an incorrect thermocouple calibration table [62Buc]). The assessed temperature is 1493 °C from [79Sch1], which is 43 °C below the melting point of Fe.

The solvus line *S′E′* was measured by [07Cha], [09Gut], [11Rue], [31Soh], [42Gur], [51Dar], [58Gen], [59Heu], [61Ben], [61Sch1], [70Ban], and [71Wad] (Fig. 5). In this evaluation, the line *S′E′* is drawn by connecting *S′* of [84Oht] and *E′* of [79Sch1], following an *S′E′* slope similar to that of [84Oht] and [79Sch1].

Because the position of point *E*′ was determined experimentally as the intersection of the *JE*′ and *SE*′ lines, the composition is sensitive to small differences in the slopes of these lines and was reported variously by [04Car], [11Rue], [38Wel], [42Gur], [46Smi], [52Kit], [59Heu], and [61Sch1] at 6.0 to 8.6 at.% C. The calculated value of 9.06 at.% C given by [79Sch1] is accepted in Fig. 2 (enlarged in Fig. 5).

The(γFe) ↔ (αFe) + C eutectoid transformation temperature was found at 746 (on heating) and 720 (on cooling) [20Rue], 735 [59Heu], and 738 °C [38Wel, 61Sch1]. The composition of the point *S*′ was reported to be 3.00 [61Sch1], 3.13 [38Wel], 3.17 [20Rue], 3.48 [59Heu], and 3.83 at.% C [52Fal]. According to a thermodynamic model of [84Oht] including the ferromagnetic effect in (αFe), the coordinates of point *S*′ are 740 °C and 2.97 at.% C.

The *GS*′ solvus was measured by [1897Rob], [1899Rob], [04Car], [04Hey], [10Goe], [13Hon], [14Rum], [14Sal], [15Sal], [16Bar], [16Hon], [18Iit], [21Mau], [23Ber], [23Kon], [26Sta], [27Ess], [27Hon2], [27Hon3], [29Sat], [30Har] [37Meh], [46Smi], [49Sta], and [85Has]. [32Kor] calculated the solvus temperature using the heat capacity data of [27Obe]. The assessed *GS*′ solvus in Fig. 2 (enlarged in Fig. 5) is from [84Oht].

(αFe) Phase

The solvus *GP*′ was measured by [46Smi], [49Pen], [49Sta], [62Smi], and [85Has]. The boundary calculated by [84Oht] is accepted (Fig. 6). The solvus *P*′*Q*′ was reported by [37Adc], [46Smi], [58Pet], [59Sin], [62Smi], [67Swa], and [85Has]. [54Hil] first attempted to calculate this boundary. In this evaluation, the boundary calculated by [84Oht] including the magnetic effect is accepted (Fig. 6).

(C) Phase

The sublimation temperature of C (graphite) is 3826 °C [Massalski2].

Fe-Fe3C (Cementite) System

The Fe-Fe_3C metastable phase diagram is shown in Fig. 7.

Liquid Phase

The boundary *AB* is the same as in the Fe-C system, and the boundary *BC* is essentially the same as the *BC*′ boundary (see above).

The L ↔ (γFe) + Fe_3C eutectic reaction temperature was reported to be 1120 to 1140 [1897Rob, 1899Rob], 1110 to 1146 [04Car], 1093 to 1134 [09Gut], 1130 [14Rue, 35Umi], <1140 [25Kay], 1144 [59Heu], 1145 [17Rue, 34Piw], 1147 [51Dar, 61Ben], 1150 [61Sch1], and 1151 °C (on heating) [30Kas]. The composition of point *C* is 16.9 [06Ben, 09Gut, 17Rue], or 17.3 at.% C [20Rue]. The calculated temperature (1147 °C) and composition (17.29 at.% C) by [79Sch1] are most reliable, because they were determined consistently from all phase boundary data involved in this reaction. [84Oht] also arrived at a very similar result (Table 2).

Because of the instability of Fe_3C (see "Fe_3C" below) at high temperatures under ambient pressure, the line *CD* has been determined only by calculation. The calculated result by [79Sch1] is

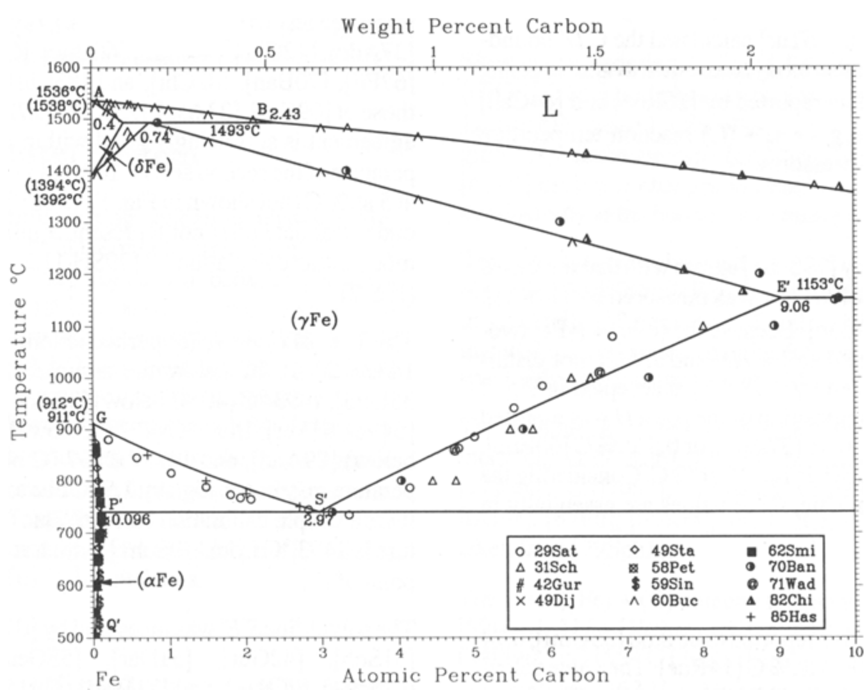

Fig. 5 (γFe) phase field of the stable Fe-C (graphite) phase diagram. Temperatures in parentheses are recommended by [Massalski2].

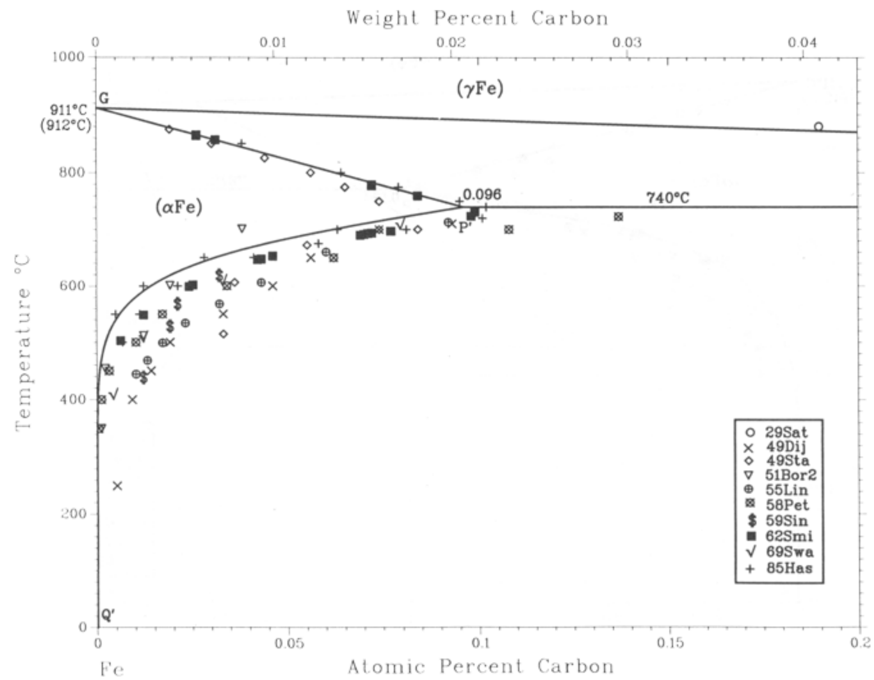

Fig. 6 (αFe) phase field of the stable Fe-C (graphite) phase diagram. Temperatures in parentheses are recommended by [Massalski2].

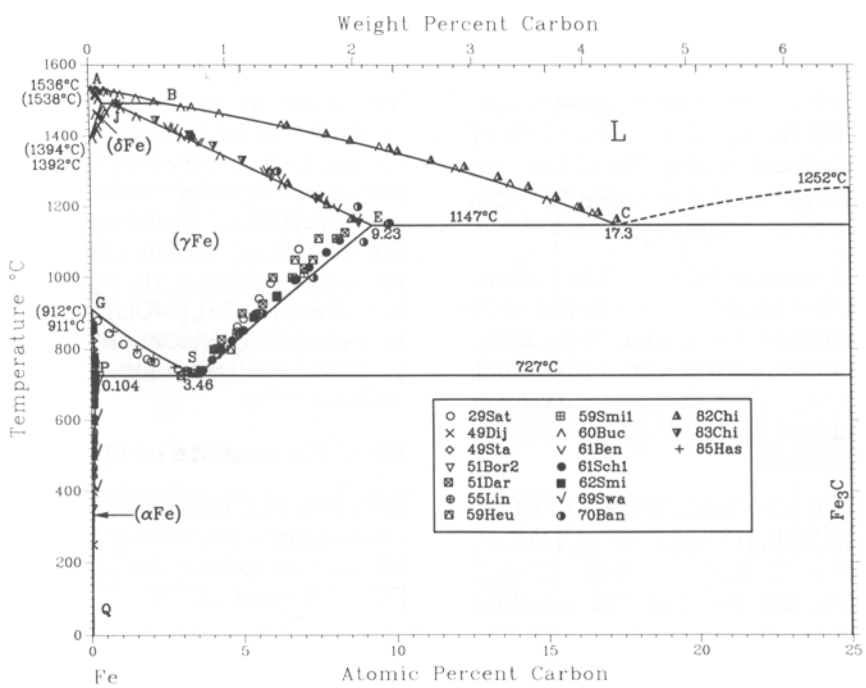

Fig. 7 Assessed Fe-Fe_3C (cementite) phase diagram. Temperatures in parentheses are recommended by [Massalski2].

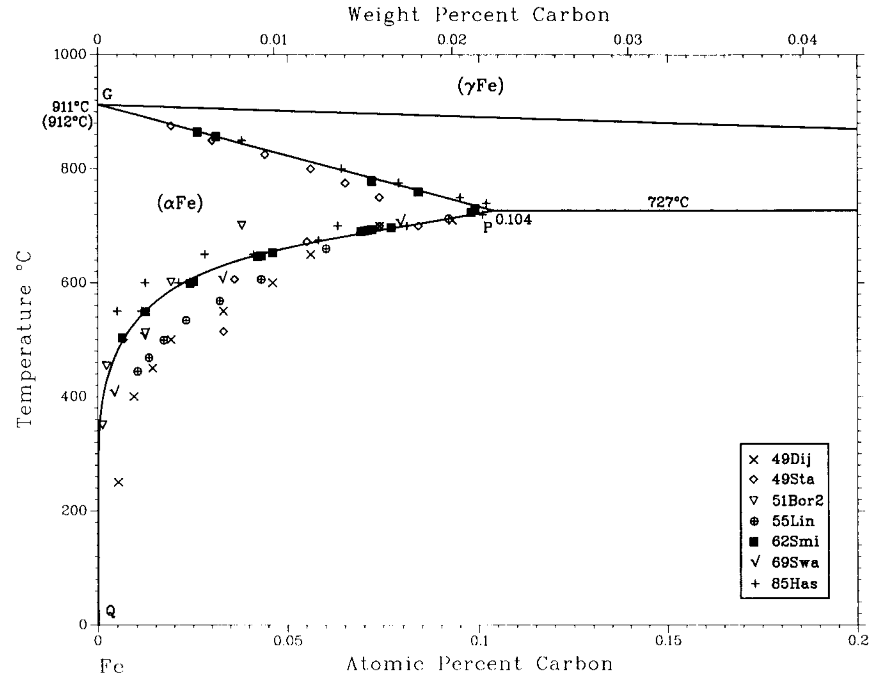

Fig. 8 (αFe) phase field of the metastable Fe-Fe_3C (cementite) phase diagram. Temperatures in parentheses are recommended by [Massalski2].

shown in Fig. 1, and that of [84Oht] is essentially identical. Earlier theoretical treatment of this boundary was reported in [55Hil].

(γFe) Phase

The (γFe) ↔ (αFe) + Fe_3C eutectoid temperature was reported to be 710 to 721.5 [16Bar], 718 [14Rum], 721 ± 3 [17Rue, 23Kon], 722 [27Ess], 723 [37Meh, 61Sch1, 64Ver], 726 [29Sat], and 727.2 ± 0.5 °C [59Smi2]. The assessed temperature is 727 °C, in agreement with the most careful work done by [59Smi2].

The composition of point *S* was reported to be 3.39 [14Rum, 21Mau], 3.44 [61Sch], 3.46 [59Smi1], 3.61 [37Meh], 3.70 [30Har], 3.83 [1897Rob, 1899Rob], 3.88 [16Hon, 26Sta, 27Ess, 29Sat], 4.01 [04Car, 14Sal, 15Sal], 4.05 [12Meu], 4.10 [23Kon], 4.18 [04Hey], and 4.27 at.% C [10Goe]. The calculated value of 3.43 at.% C by [79Sch1] is in good agreement with the most careful work by [59Smi1] and [61Sch2].

The solvus *SE* was measured by [1897Rob], [1899Rob], [04Car], [09Gut], [11War], [14Sal], [15Sal], [17Tsc], [23Kon], [25Kay], [26Sta], [27Hon2], [29Sat], [30Har], [37Meh], [51Dar], [59Heu], [59Smi1], [61Ben], and [61Sch1]. The calculated boundary represents recent data quite well (Fig. 7).

The composition of point *E* was reported to be 7.4 to 7.9 [52Fal], 8.5 [59Heu], 8.7 [61Sch1], and 9.2 at.% C [61Ben]. The calculated composition by [79Sch1] is 9.23 at.% C. Earlier theoretical treatment of this boundary was described in [51Dar].

The lines *JE* and *GS* are essentially the same as the lines *JE'* and *GS'* of the Fe-C system, respectively (see "Stable Fe-C (Graphite) System").

(αFe) Phase

The solvus *PQ* was measured by [49Dij], [49Sta], [50Wer], [51Bor2], [55Lin], [62Smi], [69Swa], and [85Has] (Fig. 8). The C concentration reported by [51Bor2] (not shown in Fig. 8) is too low because Fe_2C (see "Metastable Phases") was in equilibrium with (αFe) [55Lin]. Grain boundaries increase the solubility of C in (αFe) [55Lag]. Therefore, the apparent solubility of C is larger for smaller grain sizes. The *PQ* line was calculated theoretically by [50Wer], [72Chi], [84Oht] and [85Gus]. The result of [84Oht] is accepted in Fig. 8 because of its best agreement with recent experimental data that considered the effects of ferromagnetic interactions in (αFe).

Fe_3C (Cementite or θ)

Metastable Fe_3C decomposes at high temperatures [21Rue]. The thermodynamic properties of L and Fe_3C suggest that the unstable congruent melting point is 1252 °C [79Sch1, 84Oht], whereas [72Chi] obtained 1227 °C.

Metastable Phases

Numerous Fe-C compounds have been reported: FeC, Fe_2C, Fe_3C, Fe_3C_2, Fe_4C, Fe_5C_2, Fe_6C, Fe_7C_3, Fe_8C, $Fe_{20}C_9$, $Fe_{23}C$,

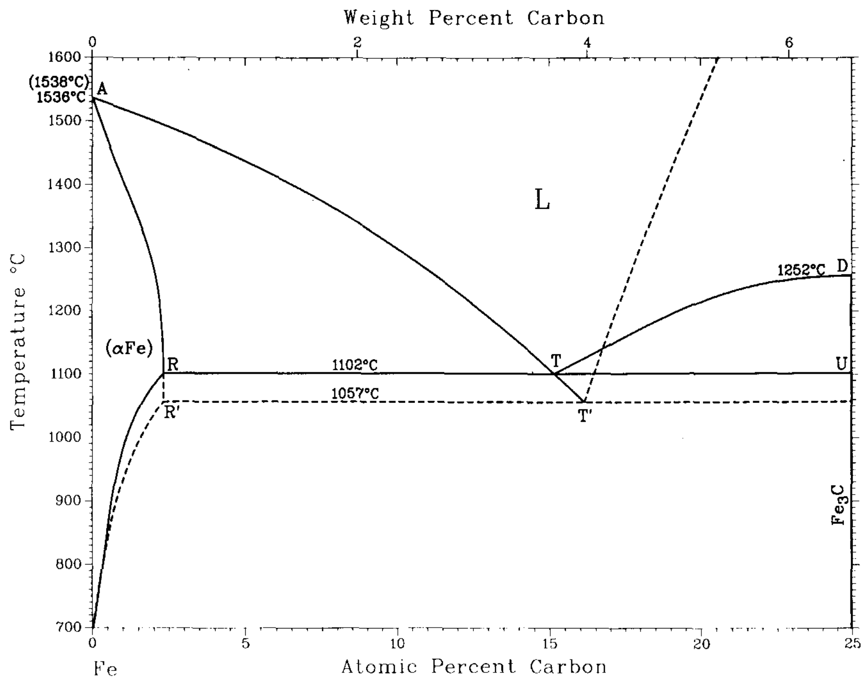

Fig. 9 Metastable αFe (ferrite)-Fe_3C (cementite) and αFe (ferrite)-C (graphite) equilibria. From [79Sch2].

and $Fe_{23}C_6$. Many are transitional phases or stabilized by impurity elements. Only those clearly defined are described here.

Martensite

Martensite is a tetragonal phase formed by rapid quenching of fcc (γFe). The martensitic transformation is *not* discussed in this evaluation.

(γFe) at Room Temperature

The fcc (γFe) phase can be retained at room temperature in very rapidly quenched alloys by suppressing the martensitic transformation temperature [78Sch, 85Tak].

Fe_4C

Cubic [56Pin, 57Pin] or hexagonal [58Ska] Fe_4C have been reported. The lack of additional evidence suggests that Fe_4C is probably a transitional phase.

Fe_3C (Cementite, θ)

The Fe-Fe_3C (cementite) system is described in the "Equilibrium Diagram" section.

Fe_5C_2 (Hägg Carbide or χ)

This phase was found by [34Häg1]. The monoclinic structure was determined by [63Sen].

Fe_7C_3

This compound is hexagonal [64Her2] or orthorhombic Fe_7C_3 [69Fru], and it is found in high-pressure Fe-C phase diagrams (see "Pressure" section). The orthorhombic structure is obtained by distorting the hexagonal structure slightly. There is a close relationship between the lattice parameters of the hexagonal and orthorhombic structures (see "Crystal Structures and Lattice Parameters" section). It is not clear whether these two structures exist at different temperatures or if only one of the two exists.

Fe_2C (ε or η)

A transient phase Fe_2C with hexagonal (ε) or orthorhombic (η) structure has been reported repeatedly by [29Glu], [30Hof], [33Bah], [40Arb], [46Jac], [47Isa], [48Jac], [49Hof], [50Jac], [53Coh], [56Nag], [57Gud], [58Mar], [59Nag], and [68Dug]. Because of uncertainty in the composition, this phase was also called εFe_3C. [72Hir] established that the structure of Fe_2C is an orthorhombic distortion of hexagonal ε; this was confirmed by [79Wil], [81Tan], and [83Kap].

$Fe_{20}C_9$ was proposed by [48Jac] instead of Fe_2C, but [59Nag] could not confirm its existence by an electron diffraction study.

"FeC"

"FeC" found by [50Eck] is actually hexagonal [64Her2] or orthorhombic Fe_7C_3 [69Fru].

(C) (Diamond)

The Fe-C (diamond) system is described in the "Pressure" section. Formation of various stable and metastable phases is observable also by splat quenching [69Ruh] or C implantation in Fe [81Tre, 82Dra, 89Oli].

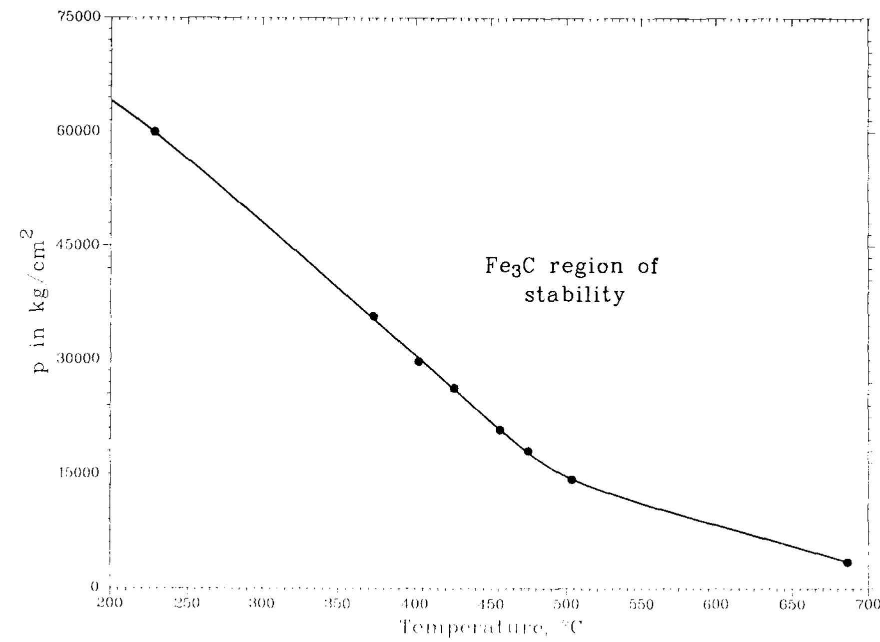

Fig. 10 Equilibrium line of the reaction $Fe_3C \leftrightarrow 3Fe + C$(graphite). From [70Ver].

Figure 9 is a summary of stable and metastable equilibria calculated by [79Sch2]. The compositions and temperatures of reactions involving (αFe) are adjusted according to [84Oht], as described above.

Pressure

Fe-Fe$_3$C System

[63Hil] investigated the effect of pressure on the (γFe) $\leftrightarrow$ (αFe) + Fe_3C eutectoid region at 35, 50, and 65 kbar. The trend agrees with that concluded from a theoretical work by [64Yer] (see "Thermodynamics" section). The stability region of Fe_3C (Fig. 10) was redrawn from [70Ver].

Fe-C (Diamond) System

Fe-C (diamond) phase diagrams were reported by [73Zhu2] and [73Zhu3] at 80 kbar (Fig. 11) and by [69Gri] at 130 kbar (Fig. 12). At 80 kbar, the C (graphite) phase should appear above ~2300 °C, according to the pressure temperature diagram of pure C given in [69Gri]. Therefore, Fig. 12 is modified accordingly. The stable solid phases are (γFe), (εFe), Fe_3C, Fe_7C_3, C (diamond), and C (graphite) at 80 kbar and (γFe), (εFe), Fe_3C, Fe_7C_3, Fe_2C, and C (diamond) at 130 kbar (see "Thermodynamics" section for stability of Fe_3C).

At ambient pressure, Fe + C (diamond) become relatively more stable than Fe + Fe_3C below 580 °C [73Zhu1]. The metastable Fe-C (diamond) phase diagram at the ambient pressure is shown in Fig. 13.

Crystal Structures and Lattice Parameters

Fe-C crystal structure data are summarized in Table 3. The lattice parameter data are given in Tables 4 and 5.

(γFe)

The composition dependence of the lattice parameter of (γFe) was measured by [31Ohm], [32Hon1], [32Hon2], [34Hag2], [49Wra], [50Maz], [52Fal], [53Rob], [69Ruh], [70Rid], and [85Tak] (Fig. 14). [70Rid] measured the temperature dependence of the lattice parameter as well (Fig. 15).

According to [53Hou], the lattice parameter of (δFe) is smaller when martensite coexists. However, this assertion has not been corroborated. C atoms occupy the octahedral sites in fcc (γFe) [30Hen, 42Pet, 62Gar], not trigonal prismatic holes [32Wes, 40Lip].

(αFe)

[24Wev], [26Fin], [27Sel], and [49Gol] observed no change in the lattice parameter of (αFe) due to the narrow solubility range. C atoms occupy interstitial sites [53Wil].

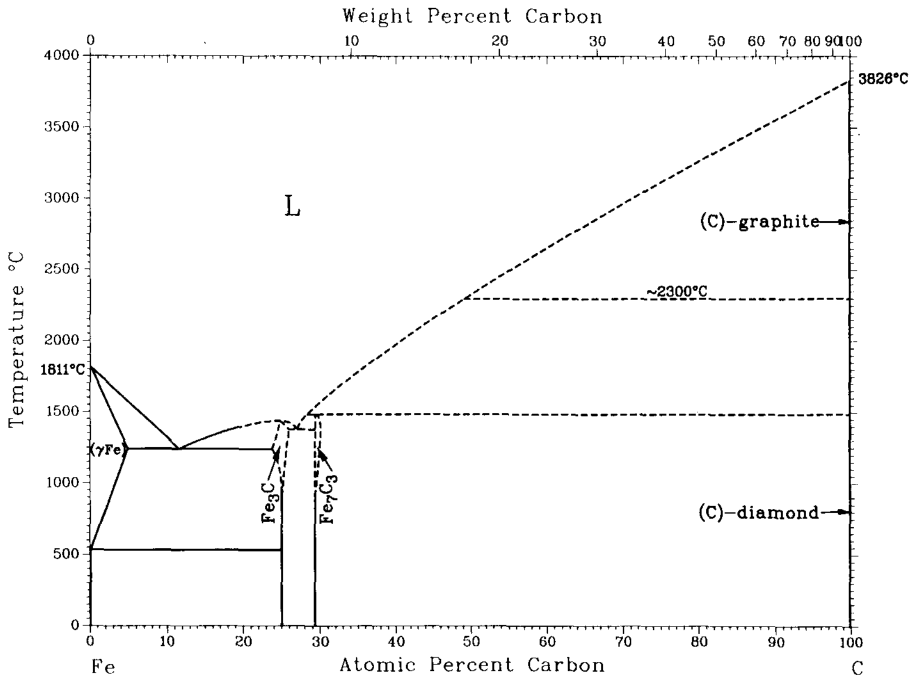

Fig. 11 Assessed Fe-C (diamond) phase diagram at 80 kbar.

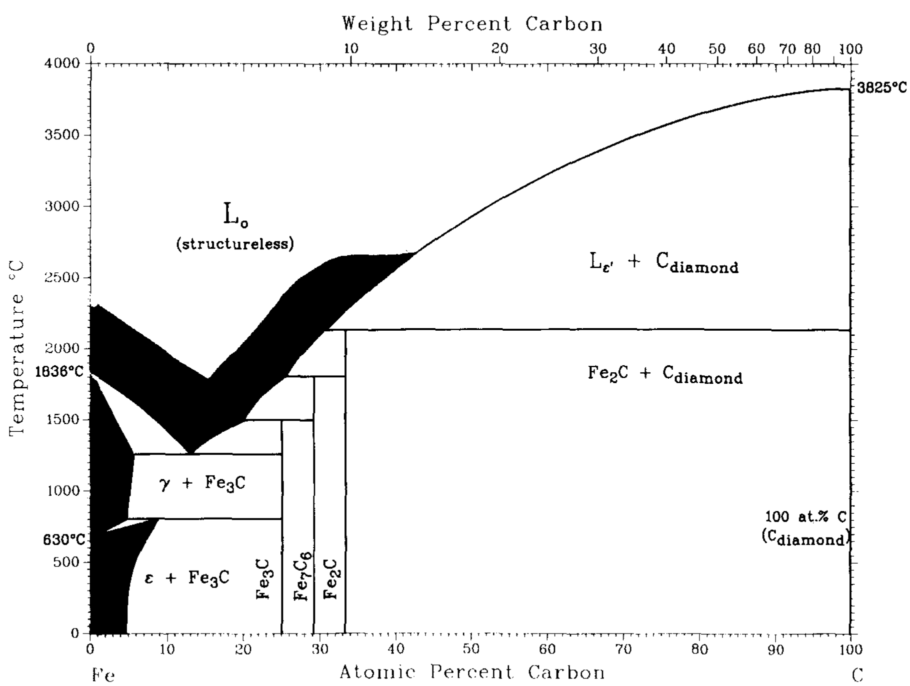

Fig. 12 Assessed Fe-C (diamond) phase diagram at 130 kbar. From [69Gri].

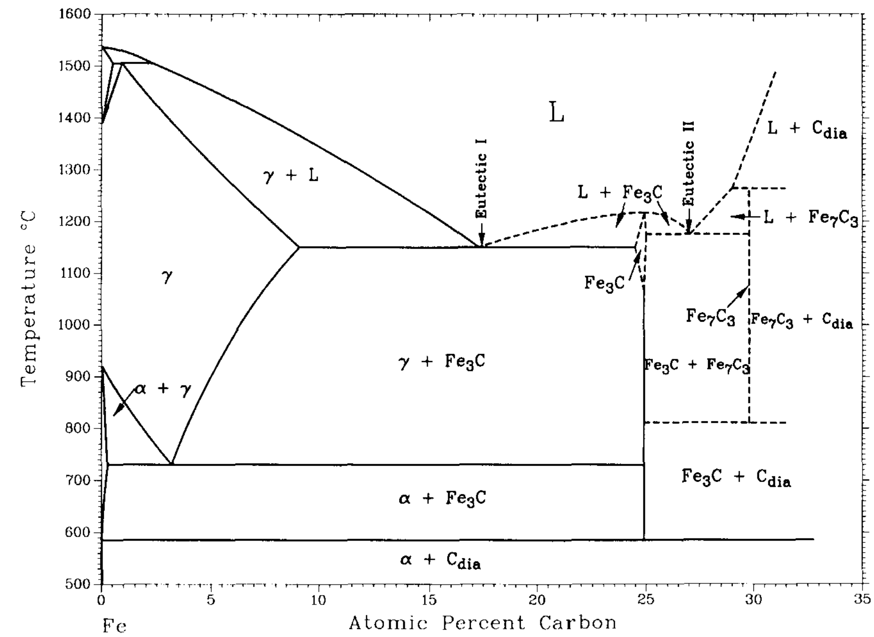

Fig. 13 Fe-C (diamond) phase diagram at ambient pressure. From [73Zhu1].

Table 3 Fe-C Crystal Structure Data

Phase	Composition, at.% C	Pearson symbol	Space group	Strukturbericht designation	Prototype	Reference
(δFe)	0 to 0.4	*cI2*	*Im*$\bar{3}$*m*	*A*2	W	[King2]
(γFe)	0 to 9.06	*cF*4	*Fm*$\bar{3}$*m*	*A*1	Cu	[King2]
(αFe)	0 to 0.096	*cI2*	*Im*$\bar{3}$*m*	*A*2	W	[King1]
(C)	100	*hP*4	*P*6$_3$/*mmc*	*A*9	C (graphite)	[King1]
Metastable/high-pressure phases						
(εFe)	0	*hP*2	*P*6$_3$/*mmc*	*A*3	Mg	[82Swa]
Martensite	<9	*tI*4	*I*4/*mmm*	*L*′2	...	[43Pet]
Fe_4C	20	*cP*5	*P*$\bar{4}$3*m*	...	...	[56Pin]
Fe_3C(θ)	25	*oP*16	*Pnma*	*D*0$_{11}$	Fe_3C	[28Wes]
Fe_5C_2(χ,Hägg)	28.6	*mC*28	*C*2/*c*	...	...	[66Jac]
Fe_7C_3	30	*hP*20	*P*6$_3$*mc*	*D*10$_2$	Fe_3Th_7	[64Her2]
Fe_7C_3	30	*oP*40	*Pnma*	...	...	[69Fru]
Fe_2C(η)	33.3	*oP*6	*Pnnm*	...	...	[72Hir]
Fe_2C(ε)	33.3	*hP**	*P*6$_3$22	...	...	[50Jac]
Fe_2C	33.3	*hP**	*P*$\bar{3}$*m*1	...	...	[68Dug]
(C)	100	*cF*8	*Fd*$\bar{3}$*m*	*A*4	C(diamond)	[King2]

Martensite

The composition dependence of the lattice parameters is shown in Fig. 16 from data provided by [27Sel], [28Kur], [29Sek], [31Ohm], [32Hon1], [34Hag2], [44Lip], [46Kur], [50Arb], [50Maz], [76Kur], and [83Nag].

Structure changes of martensite on aging at room temperature and higher temperatures have been studied extensively. Although the course of transition depends on C concentration and heat treatment procedures, the transition occurs in the order: cluster formation → ε or ηFe_2C → χFe_5C_2 → θFe_3C as studied by the Möss-

Table 4 Fe-C Lattice Parameter Data of Stable Phases

Phase	Composition, at.% C	Lattice parameters, nm a	b	c	Comment	Reference
δFe	0	0.29315	...	...	At 1394 °C	[Massalski2]
(γFe)	0	0.36467	...	...	At 915 °C	[King2]
	0	0.3574	...	...	From graph	[70Rid]
	1.47	0.3582	...	...	From graph	[70Rid]
	2.03	0.35750	...	...	...	[49Wra]
	2.06	0.35752	...	...	...	[50Maz]
	2.28	0.35777	...	...	...	[49Wra]
	2.73	0.35822	...	...	...	[49Wra]
	2.82	0.3595	...	...	From graph	[70Rid]
	3.17	0.35867	...	...	...	[49Wra]
	3.22	0.3588	...	...	...	[31Ohm]
	3.39	0.35888	...	...	...	[50Maz]
	3.61	0.3591	...	...	...	[31Ohm]
	3.61	0.35912	...	...	...	[49Wra]
	3.66	0.3592	...	...	...	[32Hon1]
	3.88	0.3602	...	...	From graph	[70Rid]
	4.01	0.35951	...	...	...	[50Maz]
	4.05	0.35957	...	...	...	[49Wra]
	4.05	0.35956	...	...	...	[50Maz]
	4.18	0.3595	...	...	...	[32Hon1]
	4.49	0.36003	...	...	...	[49Wra]
	4.5	0.3593	...	...	...	[52Fal]
	4.57	0.3604	...	...	From graph	[70Rid]
	4.66	0.3599	...	...	...	[31Ohm]
	4.92	0.36048	...	...	...	[49Wra]
	4.96	0.3605	...	...	...	[32Hon1]
	5.05	0.36094	...	...	...	[69Ruh]
	5.22	0.3612	...	...	From graph	[70Rid]
	5.35	0.3607	...	...	...	[31Ohm]
	5.35	0.36093	...	...	...	[49Wra]
	5.56	0.36116	...	...	...	[50Maz]
	5.69	0.3614	...	...	...	[32Hon1]
	5.77	0.36138	...	...	...	[49Wra]
	5.90	0.3616	...	...	...	[31Ohm]
	6.19	0.3623	...	...	...	[31Ohm]
	6.19	0.36183	...	...	...	[49Wra]
	6.36	0.3619	...	...	From graph	[70Rid]
	6.61	0.36228	...	...	...	[49Wra]
	6.9	0.3642	...	...	...	[52Fal]
	7.03	0.36273	...	...	...	[49Wra]
	7.3	0.3634	...	...	...	[52Fal]
	7.32	0.36270	...	...	...	[69Ruh]
	7.44	0.36318	...	...	...	[49Wra]
	7.61	0.3630	...	...	...	[32Hon1]
	7.76	0.36354	...	...	...	[49Wra]
	8	0.363	...	...	...	[85Tak]
	8.18	0.36338	...	...	...	[69Ruh]
αFe	0	0.28655	...	...	...	[King1]
C	100	0.24612	...	...	...	[King1]

bauer effect [68Ino, 83Kap] and by electron microscopy [83Nag]. [43Pet] determined the position of C atoms in martensite.

εFe_2C

See the "Metastable Phases" section.

θFe_3C (Cementite)

Determination of the structure of cementite was attempted repeatedly [22Wes1, 22Wes2, 23Wev, 28Wes, 29Shi, 30Hen, 32Wes, 40Lip]. The currently accepted structure was reported by [28Wes]. Neutron diffraction data were given in [62Mei] and [63Lya], and electron diffraction data were reported in [62Gar].

The lattice parameters of Fe_3C were measured by several investigators (Table 5). Among considerably scattered data, the values given by [40Lip], [42Hum], and [44Pet] are most consistent. [71Gac] measured the temperature dependence of the lattice parameters in the range from –200 to 500 °C and obtained

$$a = 0.45198(1 + 4.11 \times 10^{-6}T + 12.1 \times 10^{-9}T^2)\ \text{nm}$$
$$b = 0.50845(1 + 0.98 \times 10^{-6}T + 15.3 \times 10^{-9}T^2)\ \text{nm}$$
$$c = 0.67384(1 + 13.5 \times 10^{-6}T + 2.1 \times 10^{-9}T^2)\ \text{nm}$$

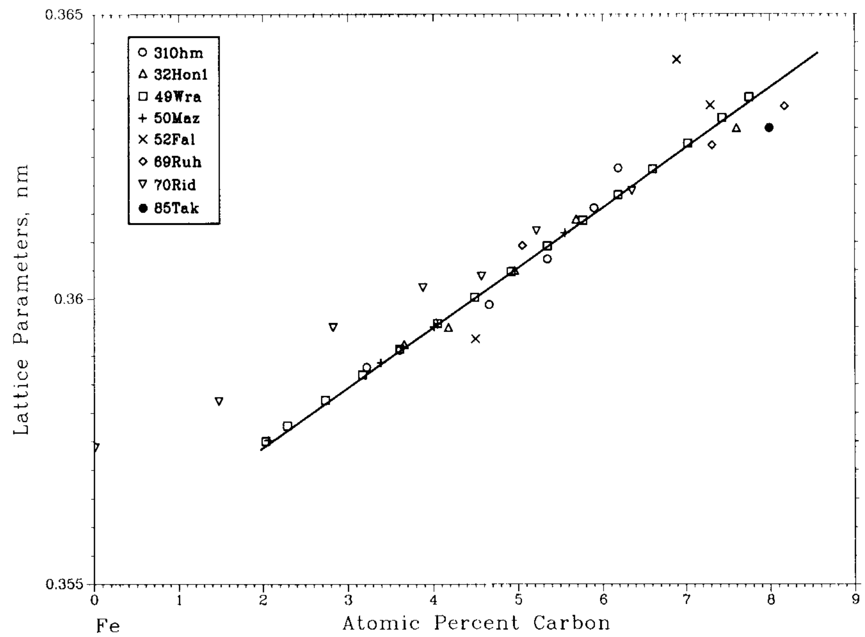

Fig. 14 Composition dependence of the lattice parameter of (γFe).

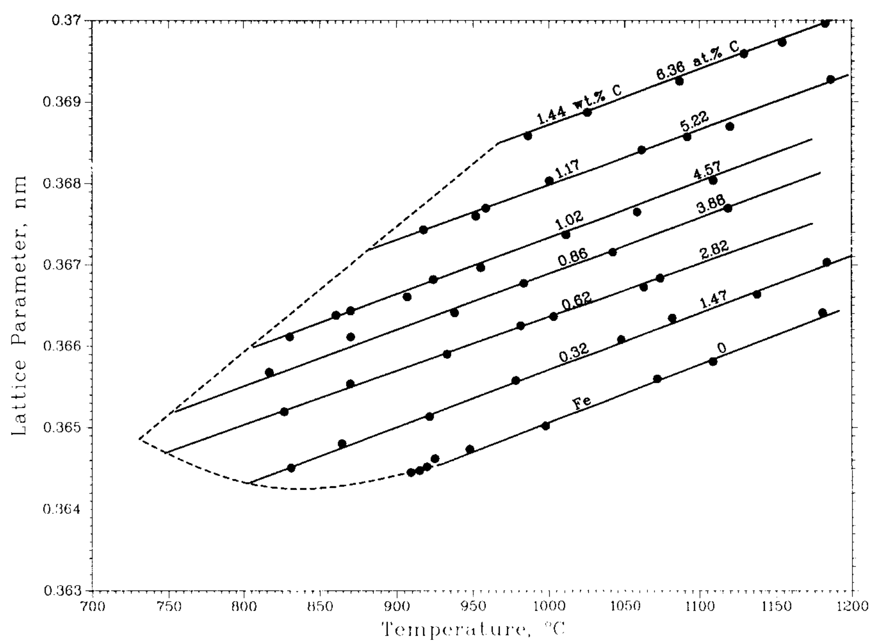

Fig. 15 Temperature dependence of the lattice parameter of (γFe) containing up to 6.36 at.% C. From [70Rid].

Table 5 Fe-C Lattice Parameter Data of Metastable/High-Pressure Phases

Phase	Composition, at.% C	Lattice parameters, nm a	b	c	Comment	Reference
εFe	0	0.2468	...	...	At 13 GPa	[Massalski2]
Martensite	2.69	0.2858	...	0.2935	...	[32Hon1]
	2.91	0.2856	...	0.2927	...	[28Kur]
	3.22	0.2853	...	0.2947	...	[31Ohm]
	3.39	0.2856	...	0.2945	...	[50Maz]
	3.44	0.2855	...	0.2949	...	[28Kur]
	3.61	0.2858	...	0.2962	...	[31Ohm]
	3.66	0.2853	...	0.2962	...	[32Hon1]
	4.01	0.2855	...	0.2968	...	[50Maz]
	4.05	0.2853	...	0.2969	...	[50Maz]
	4.10	0.2853	...	0.2953	...	[28Kur]
	4.18	0.2850	...	0.2975	...	[32Hon1]
	4.62	0.2851	...	0.2973	...	[28Kur]
	4.66	0.2854	...	0.2985	...	[31Ohm]
	4.96	0.2852	...	0.2993	...	[32Hon1]
	5.26	0.2849	...	0.2985	...	[28Kur]
	5.35	0.2852	...	0.3005	...	[31Ohm]
	5.35	0.2849	...	0.3011	...	[50Maz]
	5.56	0.2848	...	0.3014	...	[50Maz]
	5.69	0.2852	...	0.3019	...	[32Hon1]
	5.90	0.2849	...	0.3020	...	[31Ohm]
	6.07	0.2847	...	0.3003	...	[28Kur]
	6.19	0.2846	...	0.3040	...	[31Ohm]
	6.2	0.2852	...	0.303	...	[46Kur]
	6.36	0.2846	...	0.3011	...	[28Kur]
Fe_4C	20	0.3878	...	...	...	[56Pin]
$Fe_3C(\theta)$	25	0.4526	0.5089	0.6744	...	[22Wes2]
		0.4527	0.5079	0.6750	...	[30Hen]
		0.45235	0.50890	0.67433	At 21 °C	[40Lip]
		0.45246	0.50876	0.67401	At 25 °C	[42Hum]
		0.45230	0.50890	0.67428	At 18.9 °C	[44Pet]
		0.45244	0.50885	0.67431	...	[48Jac]
		0.4514	0.5084	0.6746	...	[49Gol]
		0.451	0.5079	0.6730	...	[56Pop]
		0.4526	0.5087	0.6744	...	[57Fru]
		0.4525	0.5087	0.6741	...	[59Nag]
		0.45255	0.5089	0.6744	...	[61Stu]
		0.4516	0.5077	0.6727	...	[62Oke]
		0.4523	0.5090	0.6748	...	[64Her1]
$Fe_5C_2(\chi)$	28.6	1.1563	0.4573	0.5058	β = 97.73 (a)	[63Sen]
		1.156	0.456	0.503	β = 98.05	[66Dug]
		1.1562	0.45727	0.50595	β = 97.74	[66Jac]
Fe_7C_3	30	0.6882	...	0.4540	...	[64Her2]
	30	0.4540	0.6879	1.1942	...	[69Fru]
$Fe_2C(\eta)$	33.3	0.4704	0.4318	0.2830	...	[72Hir]
		0.470	0.429	0.285	...	[81Tan]
$Fe_2C(\varepsilon)$ (b)	33.3	0.274	...	0.434	...	[50Jac]
		0.2754	...	0.4349	...	[53Coh]
		0.2756	...	0.4362	...	[59Nag]
		0.2752	...	0.4354	...	[62Oke]
		0.2794	...	0.4360	(c)	[64Bar]
		0.2750	...	0.4353	...	[68Dug]
C(diamond)	100	0.35669	...	...	...	[Massalski2]

(a) Slightly different values were reported by the same author [62Sen,67Sen]. (b) Actual structure is orthorhombic. (c) Monoclinic distortion.

where T is in °C. These equations give slightly lower values at room temperature than those given by [40Lip], [42Hum], and [44Pet].

The lattice parameters at room temperature vary depending on the quenching temperature [44Pet]. For example, the lattice parameters a, b, and c of a specimen quenched from 900 °C differ by −0.00067, −0.00052, and +0.00047 nm from those of a slowly cooled specimen.

Fe_5C_2

Monoclinic lattice parameters measured by [63Sen] and [66Jac] are in agreement.

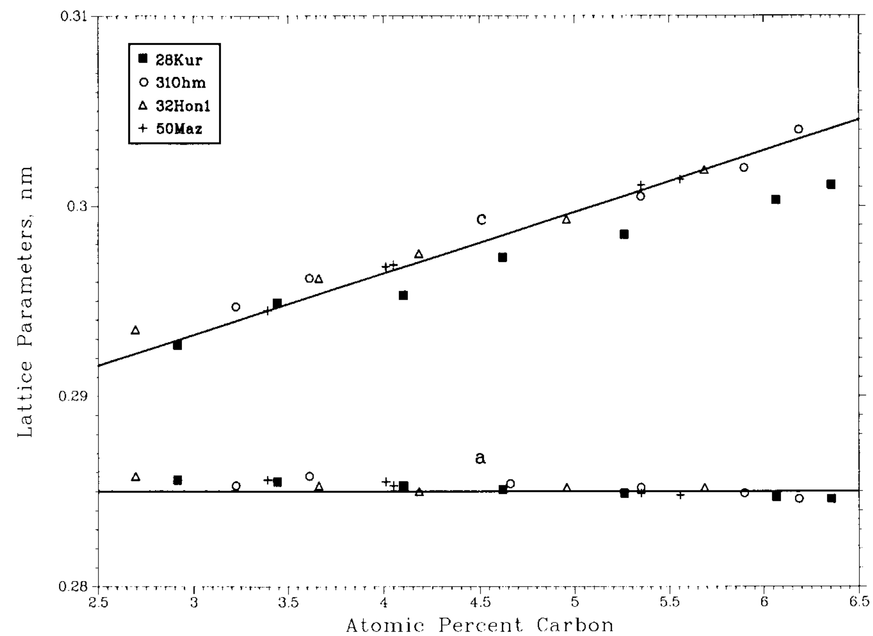

Fig. 16 Composition dependence of the lattice parameters of martensite.

Fe_7C_3

Both hexagonal [64Her2] and orthorhombic [69Fru] lattice parameters are listed in Table 5. Apparently, *a*(ort) = *c*(hex), *b*(ort) = *a*(hex), and *c*(ort) = $\sqrt{3}a$(hex).

η and ε Fe_2C

Although hexagonal ε is actually distorted to an orthorhombic form η (see "Metastable Phases"), the lattice parameters are listed as reported in Table 5. Approximately, *a*(ort) = $\sqrt{3}a$(hex), *b*(ort) = *c*(hex), and *c*(ort) = *a*(hex).

Thermodynamics

Thermodynamic data available on the Fe-C system are numerous. Important sources for thermodynamic modeling of the phase diagram are [42Mar], [53Ric], [53San], [56Ris], [59Fuw], [59Syu], [63Fel], [68Mor], [68Wad], [69Ban], [70Chi], [72Yav], and [79Sch1] for activity data of the liquid phase and [31Dun], [46Smi], [49Tem], [57Vin], [60Sch], [61Sch2], [64Bun], [64Sch], [65Hud], [68Haw], [69Ban], and [70Ban] for activity data of the (γFe) phase.

Thermodynamic modeling of the Fe-C phase diagram has been attempted by many investigators [50Wer, 51Sch, 53Dar, 53Ric, 54Hil, 55Hil, 56Ris, 56Tur, 61Ben, 63Fel, 67Orr, 68Bur, 68Fis, 68Shv, 70Chi, 71Har, 72Chi, 74Bas, 79Agr, 79Sch1, 79Sch2, 84Oht, 85Gus, 85Has]. Recent extensive studies by [79Sch1] based on a short-range order model and by [84Oht] based on a regular-solution sublattice model differ only slightly—<0.2 at.% and <1 °C, except for the phase boundaries of magnetic (αFe)—in the form of the calculated diagrams (Table 2).

[64Yer] calculated the influence of pressure (up to 50 kbar) on the (γFe) ↔ (αFe) + (C) and (γFe) ↔ (αFe) + Fe_3C eutectoid regions and showed that the eutectoid points shift toward lower temperatures and lower C concentrations at high pressures. According to the pressure-temperature diagram calculated by [63Ers], Fe-Fe_3C becomes the stable system at pressures higher than 2 kbar near the L ↔ (γFe) + Fe_3C eutectic temperature.

Magnetism

The Curie temperature of αFe is 770 °C [82Swa]. The composition dependence could not be detected [24Wev, 26Fin, 27Sel] because of the narrow homogeneity range of (αFe). The Curie temperature of Fe_3C was reported at 210 [12Smi, 15Hon, 17Ish, 22Tam, 27Tam, 37Tra], 212 ± 3 [53Coh], 214 [61Stu], and 215 °C [17Hon, 28Leh, 28Mit]. The Curie temperatures of transient phases are 380 °C for Fe_2C [53Coh], 247 °C for Fe_5C_2 [53Coh, 66Hof], and 250 °C for Fe_7C_3 [66Hof].

Cited References

1897Rob: W.C. Roberts-Austen, "Fourth Report to the Alloys Research Committee," *Proc. Inst. Mech. Eng.*, 31-100 (1897). (Equi Diagram; Experimental; #)

1899Rob: W.C. Roberts-Austen, "Fifth Report to the Alloys Research Committee: Steel," *Proc. Inst. Mech. Eng.*, 35-102 (1899). (Equi Diagram; Experimental; #)

00Bak: H.W. Bakhuis Roozeboom, "Iron and Steel from the Standpoint of Phase Rule," *Z. Phys. Chem.*, *34*, 437-487 (1900) in German. (Equi Diagram; Experimental; #)

04Car: H.C.H. Carpenter and B.F.E. Keeling, "The Range of Solidification and the Critical Ranges of Iron Carbon Alloys," *J. Iron Steel Inst.*, *65*, 224-242 (1904). (Equi Diagram; Experimental; #)

04Hey: E. Heyn, "Unstable and Metastable Equilibrium in Iron-Carbon Alloys," *Z. Elektrochem.*, *10*(30), 491-504 (1904) in German. (Equi Diagram; Experimental; #)

06Ben: C. Benedicks, "Equilibrium and Solidification Structures of the Iron-Carbon System," *Metallurgie*, *3*(12), 393-395; *3*(13), 425-441; *3*(14), 466-476 (1906) in German. (Equi Diagram; Experimental)

07Cha: G. Charpy, "Solubility of Graphite in Iron," *Compt. Rend.*, *145*(25), 1277-1279 (1907) in French; *Rev. Metall.*, *5*(2), 77-78 (1908) in French. (Equi Diagram; Experimental)

09Gut: N. Gutowski, "Theory of Melting and Solidification Processes of Iron-Carbon Alloys," *Metallurgie*, *6*(22), 731-736 (1909) in German; abstr: *Stahl Eisen*, *29*(52), 2066-2068 (1909) in German. (Equi Diagram; Experimental; #)

10Goe: P. Goerens and H. Meyer, "Determination of Transformation Lines of γ Iron in β- or α-Iron," *Metallurgie*, *7*(10), 307-312 (1910) in German. (Equi Diagram; Experimental; #)

11Han: H. Hanemann, "Carbon Contents and Structural Appearance of Iron-Carbon Alloys High in Carbon," *Stahl Eisen*, *31*(9), 333-336 (1911) in German. (Equi Diagram; Experimental; #)

11Rue: R. Ruer and N. Iljin, "Study on Stable Iron-Carbon System," *Metallurgie*, *8*(4), 97-101 (1911) in German. (Equi Diagram; Experimental; #)

11Ruf: O. Ruff and O. Goecke, "Solubility of Carbon in Iron," *Metallurgie*, *8*(14), 417-421 (1911) in German. (Equi Diagram; Experimental)

11War: N.J. Wark, "Determination of Solubility of Iron Carbide (Fe_3C) in γ-Iron," *Metallurgie*, *8*(22), 704-713 (1911) in German; abstr: *Stahl Eisen*, *31*, 2108-2109 (1911) in German. (Equi Diagram; Experimental; #)

12Meu: A. Meuthen, "Calorimetric Investigation of the Iron-Carbon System," *Ferrum*, *10*(1), 1-21 (1912-1913) in German. (Equi Diagram; Experimental; #)

12Smi: S.W.J. Smith, "The Thermomagnetic Study of Steel," *Proc. Phys. Soc. (London)*, *25*, 77-81 (1912). (Magnetism; Experimental)

12Wit: N.F. Wittorf, "Preliminary Investigation on Primary Crystallization and Subsequent Physicochemical Transformations in the Iron-Carbon System Containing More Than 4% Carbon, *Z. Anorg. Chem.*, *79*(1), 1-70 (1912) in German. (Equi Diagram; Experimental; #)

13Hon: K. Honda, "Thermomagnetic Properties of Iron and Steel," *Sci. Rep. Tohoku Univ.*, *2*, 203-216 (1913) in German. (Equi Diagram; Experimental; #)

14Rue: R. Ruer and R. Klesper, "The γδ Transformation of Pure Iron and Influence of Carbon, Silicon, Cobalt, and Copper on It," *Ferrum*, *11*(9), 257-261 (1913-1914) in German. (Equi Diagram; Experimental; #)

14Ruf: O. Ruff and W. Bormann, "Studies in a High Temperature Region. VII. Iron and Carbon," *Z. Anorg. Chem.*, *88*(4), 397-409 (1914) in German. (Equi Diagram; Experimental; #)

14Rum: G. Rumelin and R. Maire, "The Magnetic Transitions in Iron-Carbon Alloys," *Ferrum*, *12*, 141-154 (1914-1915) in German. (Equi Diagram; Experimental; #)

14Sal: P. Saldau and P. Goerens, "Determination of the Curve of Transformation of γ Iron into α and β Iron and of the Curve of Saturation of γ Iron by Cementite," *Zh. Russ. Met. Obshch.*, (1), 789-824 (1914) in Russian; abstr.: *Stahl. Eisen*, *38*, 15-17 (1918). (Equi Diagram; Experimental; #)

15Hon: K. Honda and H. Takagi, "On the Magnetic Transformation of Cementite," *Sci. Rep. Tohoku Univ.*, *4*, 161-168 (1915). (Magnetism; Experimental)

15Sal: P.J. Saldau, "A New Line in the Iron-Carbon Diagram at 980 °C (in the Austenite) Region and Tchernoff's Point 'b'," *Zh. Russ. Met. Obshch.*, 655-690 (1915), 78-80 (1916) in Russian; abstr.: *Stahl. Eisen*, *38*, 39-40 (1918). (Equi Diagram; Experimental; #)

16Bar: P. Bardenheuer, "Critical Points of Pure Carbon Steels," *Ferrum*, *14*, 129-133, 145-151 (1916) in German. (Equi Diagram; Experimental; #)

16Hon: K. Honda, "On the Temperature of the Reversible A_1 Transformation in Carbon Steels," *Sci. Rep. Tohoku Univ.*, *5*, 285 (1916). (Equi Diagram; Experimental; #)

17Hon: K. Honda and T. Murakami, "On the Thermomagnetic Properties of the Carbides Found in Steels," *Sci. Rep. Tohoku Univ.*, *6*, 23-29 (1917). (Magnetism; Experimental)

17Ish: T. Ishiwara, "On the Magnetic Analysis of Carbides Found in Different Kind of Steel," *Sci. Rep. Tohoku Univ.*, *6*, 285-294 (1917). (Magnetism; Experimental)

17Rue: R. Ruer and F. Goerens, "The Process of Melting and Freezing in Iron-Carbon Alloys," *Ferrum*, *14*, 161-177 (1917) in German. (Equi Diagram; Experimental; #)

17Tsc: N. Tschischewsky and N. Schulgin, "The Determination of the Line SE in the Iron Carbon Diagram by Etching Sections at High Temperatures in Vacuo," *J. Iron Steel Inst.*, *95*, 189-198 (1917). (Equi Diagram; Experimental; #)

18Iit: I. Iitaka, "A Study of Cementite Transformation and of the Equilibrium Diagram of the System Iron-Carbon by Means of Electric Resistance Measurements," *Sci. Rep. Tohoku Univ.*, *7*, 167-175 (1918). (Equi Diagram; Experimental)

20Rue: R. Ruer and J. Biren, "On the Solubility of Graphite in Molten Iron," *Z. Anorg. Allg. Chem.*, *113*, 98-112 (1920) in German. (Equi Diagram; Experimental; #)

21Mau: E. Mauer, quoted in *Stahl Eisen*, *41*, 1696-1706 (1921) in German. (Equi Diagram; Experimental; #)

21Rue: R. Ruer, "Iron-Carbon Alloys," *Z. Anorg. Chem.*, *117*, 249-261 (1921) in German. (Equi Diagram; Experimental; #)

22Tam: G. Tammann and K. Ewig, "Transformation of Cementite at 210°," *Stahl Eisen*, *42*(20), 772-775 (1922) in German. (Magnetism; Experimental)

22Wes1: A. Westgren and G. Phragmen, "Crystal Structure of Iron and Steel. II," *Z. Phys. Chem.*, *103*, 1-25 (1922) in German. (Crys Structure; Experimental)

22Wes2: A. Westgren and G. Phragmen, "X-Ray Studies on the Crystal Structure of Steel," *J. Iron Steel Inst.*, *105*(1), 241-262 (1922). (Crys Structure; Experimental)

23Asa: G. Asahara, "The Solidus Curve of Austenite," *Bull. Inst. Phys. Chem. Res. (Tokyo)*, *2*, 420-425 (1923). (Equi Diagram; Experimental; #)

23Ber: J.F.T. Berliner, "Preparation and Properties of Pure Iron. IV. Determination of the Critical Ranges of Pure Iron-Carbon Alloys by the Thermoelectric Method," *NBS Sci. Papers 484*, *19*, 347-356 (1923-1924). (Equi Diagram; Experimental)

23Kon: S. Konno, "A Study of the A_1 and A_3 Transformations in Carbon Steels by Means of a Differential Dilatometer," *Sci. Rep. Tohoku Univ.*, *12*, 127-136 (1923). (Equi Diagram; Experimental; #)

23Wev: F. Wever, "Iron Carbide," *Mitt. Kaiser Wilhelm Inst. Eisenforsch.*, *4*, 67-80 (1923) in German. (Crys Structure; Experimental)

24Wev: F. Wever, "Constitution of Technical Iron," *Z. Elektrochem.*, *30*, 376-382 (1924). (Crys Structure, Magnetism; Experimental)

25Kay: S. Kaya, "On the Solidus Line in the Iron-Carbon System," *Sci. Rep. Tohoku Univ.*, *14*, 529-536 (1925). (Equi Diagram; Experimental; #)

26Ell: O.W. Ellis, "An Investigation into the Effect of Constitution on the Malleability of Steel at High Temperatures," *Iron Steel Inst., Carnegie Schol. Mem.*, *15*, 195-215 (1926). (Equi Diagram; Experimental; #)

26Fin: W.L. Fink and E.D. Campbell, "Influence of Heat Treatment and Carbon Contents on the Structure of Pure Iron-Carbon Alloys," *Trans. ASST*, *9*, 717-748 (1926). (Crys Structure, Magnetism; Experimental)

26Sta: F. Stablein, "Simple Expansion Apparatus for High Temperatures; Expansion Behavior of Carbon Steels in the Transition Range," *Stahl Eisen*, *46*, 101-104 (1926) in German. (Equi Diagram; Experimental; #)

27Ess: H. Esser, "Dilatometric and Magnetic Investigation of Pure Iron and Iron-Carbon Alloys," *Stahl Eisen*, *47*(9), 337-344 (1927) in German. (Equi Diagram; Experimental; #)

27Hon1: K. Honda and H. Endo, "Magnetic Analysis As a Means of Studying the Structure of Non-Magnetic Alloys," *J. Inst. Met.*, *37*, 29-49 (1927). (Equi Diagram; Experimental; #)

27Hon2: K. Honda and H. Endo, "On the Magnetic Determination of the Solidus and Solubility Lines in the Iron-Carbon System," *Sci. Rep. Tohoku Univ.*, *16*, 235-244 (1927). (Equi Diagram; Experimental; #)

27Hon3: K. Honda and H. Endo, "On the Magnetic Susceptibility of the Iron-Carbon Alloys at High Temperatures, and the Equilibrium Diagram of the System," *Sci. Rep. Tohoku Univ.*, *16*, 627-637 (1927). (Equi Diagram; Experimental; #)

27Obe: P. Oberhoffer and W. Grosse, "Specific Heat of Iron," *Stahl Eisen*, *47*, 576-582 (1927) in German. (Equi Diagram; Experimental)

27Sel: N. Seljakov, G. Kurdjumov, and N. Goodtzov, "An X-Ray Investigation of the Structure of Carbon Steels," *Z. Phys.*, *45*, 384-408 (1927) in German. (Crys Structure, Magnetism; Experimental)

27Tam: G. Tammann and K. Ewig, "Iron Carbide (FeC_3)," *Z. Anorg. Chem.*, *167*, 384-400 (1927) in German. (Magnetism; Experimental)

28Kur: G. Kurdjumov and E. Kaminski, "X-Ray Studies of the Structure of Quenched Carbon Steel," *Nature*, *122*, 475-476 (1928). (Crys Structure; Experimental)

28Leh: E. Lehrer, *Z. Tech. Phys.*, *9*, 142 (1928); quoted in [Hansen]. (Magnetism; Experimental)

28Mit: A. Mittasch and E. Kuss, "Ammonia Synthesis with Catalysts Derived from Complex Cyanides of Iron" *Z. Elektrochem.*, *34*(4), 167-170 (1928) in German. (Magnetism; Experimental)

28Wes: A. Westgren, G. Phragmen, and T. Negresco, "On the Structure of the Iron-Chromium-Carbon System," *J. Iron Steel Inst.*, *117*, 383-400 (1928). (Crys Structure; Experimental)

29And: J.H. Andrew and D. Binnie, "The Liquidus and Solidus Ranges of Some Commercial Steels," *J. Iron Steel Inst.*, *119*, 309-346 (1929). (Equi Diagram; Experimental; #)

29Glu: W. Gluud, K.V. Otto, and H. Ritter, "Note of Formation of a Carbide Fe_2C by Reduction of Iron Oxide with Carbon Oxide at Low Temperatures," *Ber. Dtsch. Chem. Ges.*, *62*, 2483-2485 (1929) in German. (Meta Phases; Experimental)

29Jom: W.E. Jominy, "A Study of Burning and Overheating of Steel — Part II: *Trans. ASST*, *16*, 372-392 (1929). (Equi Diagram; Experimental; #)

29Sat: T. Sato, "On the Critical Points of Pure Carbon Steels," *Tech. Rep. Tohoku Univ.*, *8*, 27-52 (1929). (Equi Diagram; Experimental; #)

29Sch: K. Schichtel and E. Piwowarsky, "Influence of Alloying Elements Phosphorus, Silicon, and Nickel and the Solubility of Carbon in Liquid Iron," *Arch. Eisenhüttenwes.*, *3*(2), 139-147 (1929-1930) in German. (Equi Diagram; Experimental; #)

29Sek: S. Sekito, "The Lattice Constant of Quenched Carbon Steels," *Sci. Rep. Tohoku Univ.*, *18*, 69-77 (1929). (Crys Structure; Experimental)

29Shi: S. Shimura, "Study of the Structure of Cementite," *Proc. World Eng. Congr., Tokyo*, *34*, 223-225 (1929); *Strukturbericht*, *2*, 303-304 (1928-1932). (Crys Structure; Experimental)

30Ell: O.W. Ellis, "The Solidus of the Iron-Carbon System," *Met. Alloys*, *1*(10), 462-464 (1930). (Equi Diagram; Theory; #)

30Har: R.H. Harrington and W.P. Wood, "Critical Ranges in Pure Iron-Carbon Alloys," *Trans. ASST*, *18*, 632-654 (1930). (Equi Diagram; Experimental; #)

30Hen: S.B. Hendricks, "The Crystal Structure of Cementite," *Z. Kristallogr.*, *74*, 534-545 (1930). (Crys Structure; Experimental)

30Hof: U. Hofmann and E. Groll, "Segregation of Carbon from Carbide Oxide of Iron. III. Formation of Iron Oxides and Iron Carbides in Precipitates," *Z. Anorg. Chem.*, *191*(4), 414-428 (1930) in German. (Meta Phases; Experimental)

30Kas: T. Kase, "Formation of Graphite During the Solidification of Cast Iron," *Sci. Rep. Tohoku Univ.*, *19*, 17-35 (1930). (Equi Diagram; Experimental; #)

31Dun: H. Dunwald and C. Wagner, "Thermodynamic Investigation of the Iron-Carbon-Sulfur System," *Z. Anorg. Allg. Chem.*, *199*(4), 321-346 (1931) in German. (Thermo; Experimental)

31Ohm: E. Ohman, "X-Ray Investigations on the Crystal Structure of Hardened Steel," *J. Iron Steel Inst*, *123*, 445-463 (1931). (Crys Structure; Experimental)

31Soh: E. Sohnchen and E. Piwowarsky, "Influence of Alloying Elements Nickel, Silicon, Aluminum, and Phosphorus on the Solubility of Carbon in Liquid and Solid Iron," *Arch. Eisenhuttenwes.*, *5*(2), 111-120 (1931-1932) in German. (Equi Diagram; Experimental; #)

32Goe: P. Goerens, *Introduction to Metallography*, in German (1932). (Equi Diagram; Review)

32Hon1: K. Honda and Z. Nishiyama, "On the Nature of the Tetragonal and Cubic Martensites," *Sci. Rep. Tohoku Univ.*, *21*, 299-331 (1932). (Crys Structure; Experimental)

32Hon2: K. Honda and Z. Nishiyama, "On the Nature of the Tetragonal and Cubic Martensites," *Trans. ASST*, *20*, 464-470 (1932). (Crys Structure; Experimental)

32Kor: F. Korber and W. Oelsen, "Thermodynamic Considerations on the Equilibrium Curves of the Iron-Carbon Phase Diagram," *Arch. Eisenhuttenwes.*, *5*(11), 569-578 (1932) in German. (Equi Diagram; Theory; #)

32Wes: A. Westgren, "Crystal Structure of Cementite," *Jernkontrets Ann.*, *87*, 457-468 (1932); *Strukturbericht*, *2*, 304 (1928-1932). (Crys Structure; Experimental)

33Bah: H.A. Bahr and V. Jessen, "Fission of Carbon Oxide, on Iron Oxide and Iron," *Ber. Dtsch. Chem. Ges.*, *66*, 1238-1247 (1933) in German. (Meta Phases; Experimental)

***34Hag1:** G. Hagg, "Powder Photograph of a New Iron Carbide," *Z. Kristallogr.*, *89*, 92-94 (1934) in German. (Meta Phases; Experimental)

34Hag2: G. Hagg, "The Decomposition of Martensite," *J. Iron Steel Inst.*, *130*, 439-451 (1934). (Crys Structure; Experimental)

34Piw: E. Piwowarsky, "Displacement of Eutectic Temperature in Iron-Carbon Alloys," *Stahl Eisen*, *54*(4), 82-84 (1934) in German. (Equi Diagram; Experimental)

35Umi: S. Umino, "Specific Heat of Iron-Carbon System at High Temperatures, and the Heat Changes Accompanying Those of Phase," *Sci. Rep. Tohoku Univ.*, *23*, 720-725 (1935). (Equi Diagram; Experimental; #)

36Eps: S. Epstein, *The Alloys of Iron and Carbon*, Vol. 1, *Constitution*, McGraw-Hill, New York (1936). (Equi Diagram; Review; #)

37Adc: F. Adcock, "An Investigation of the Iron-Carbon Constitutional Diagram," *J. Iron Steel Inst.*, *135*, 281-292 (1937). (Equi Diagram; Experimental; #)

37Meh: R.F. Mehl and C. Wells, "Constitution of High-Purity Iron-Carbon Alloys," *Trans. AIME*, *125*, 429-469 (1937). (Equi Diagram; Experimental; #)

37Tra: A. Travers and R. Diebold, "Isolation of Pure Cementite by Acid Attack of Ferrous Materials and Some of Its Physical Properties," *Compt. Rend.*, *205*, 797-799 (1937) in French. (Magnetism; Experimental)

38Wel: C. Wells, "Graphitization in High Purity Iron-Carbon Alloys," *Trans. ASM*, *26*, 289-357 (1938). (Equi Diagram; Experimental; #)

40Arb: M. Arbuzov and G. Kurdjumov, "State of Carbon in Tempered Steel," *Zh. Tekh. Fiz.*, *10*, 1093-1100 (1940) in Russian; *J. Phys. USSR*, *5*(2-3), 101-108 (1941) in German. (Meta Phases; Experimental)

40Lip: H. Lipson and N.J. Petch, "The Crystal Structure of Cementite, Fe_3C," *J. Iron Steel Inst.*, *142*, 95-103 (1940). (Crys Structure; Experimental)

42Gur: R.W. Gurry, "The Solubility of Carbon as Graphite in Gamma Iron," *Trans. AIME*, *150*, 147-153 (1942). (Equi Diagram; Experimental; #)

42Hum: W. Hume-Rothery, G.V. Raynor, and A.T. Little, "The Lattice Spacings and Crystal Structure of Cementite," *J. Iron Steel Inst.*, *145*, 143-149 (1942). (Crys Structure; Experimental)

42Mar: S. Marshall and J. Chipman, "The Carbon-Oxygen Equilibrium in Liquid Iron," *Trans. ASM*, *30*, 695-746 (1942). (Thermo; Experimental)

42Pet: N.J. Petch, "The Positions of the Carbon Atoms in Austenite," *J. Iron Steel Inst.*, *145*, 111-123 (1942). (Crys Structure; Experimental)

43Pet: N.J. Petch, "The Positions of the Carbon Atoms in Martensite," *J. Iron Steel Inst.*, *147*, 221-227 (1943). (Crys Structure; Experimental)

44Lip: H. Lipson and A.M.B. Parker, "The Structure of Martensite," *J. Iron Steel Inst.*, *149*, 123-141 (1944). (Crys Structure; Experimental)

44Pet: N.J. Petch, "The Interpretation of the Crystal Structure of Cementite," *J. Iron Steel Inst.*, *149*, 143-150 (1944). (Crys Structure; Experimental)

46Jac: K.H. Jack, "Iron-Nitrogen, Iron-Carbon, and Iron-Carbon-Nitrogen Interstitial Alloys," *Nature*, *158*, 60-61 (1946). (Meta Phases; Experimental)

46Kur: G. Kurdjumov and L. Lyssak, "The Application of Single Crystals to the Study of Tempered Martensite," *Zh. Tekh. Fiz.*, *16*, 1307-1318 (1946) in Russian; *J. Iron Steel Inst.*, *156*, 29-36 (1947). (Crys Structure; Experimental)

46Smi: R.P. Smith, "Equilibrium of Iron-Carbon Alloys with Mixtures of CO-CO_2 and CH_4-H_2," *J. Am. Chem. Soc.*, *68*(7), 1163-1175 (1946). (Equi Diagram, Thermo; Experimental; #)

48Jac: K.H. Jack, "Binary and Ternary Interstitial Alloys. III. The Iron-Carbon System: the Characterization of a New Iron Carbide," *Proc. R. Soc. (London) A*, *195*, 56-61 (1948). (Meta Phases, Crys Structure; Experimental)

49Dij: L.J. Dijkstra, "Precipitation Phenomena in the Solid Solutions of Nitrogen and Carbon in Alpha Iron below the Eutectoid Temperature," *Trans. AIME*, *185*(3), 252-260 (1949). (Equi Diagram; Experimental; #)

49Gol: H.J. Goldschmidt, "Interplanar Spacings of Carbides in Steels," *Metallurgie*, *40*(6), 103-104 (1949). (Crys Structure; Experimental)

49Hof: L.J.E. Hofer, E.M. Cohn, and W.C. Peebles, "The Modifications of the Carbide, Fe_2C; Their Properties and Identification," *J. Am. Chem. Soc.*, *71*, 189-195 (1949). (Meta Phases; Experimental)

49Pen: W.A. Pennington, "Thermodynamics in the Decarburization of Steel with Mill Scale," *Trans. ASM*, *41*, 213-258 (1949). (Equi Diagram; Experimental; #)

49Sta: J.K. Stanley, "The Diffusion and Solubility of Carbon in Alpha Iron," *Trans. AIME*, *185*(10), 752-760 (1949). (Equi Diagram; Experimental; #)

49Tem: M.I. Temkin and L.A. Shvartsman, "Activity of Carbon in Austenite," *Zh. Fiz. Khim.*, (6), 7, 55 (1949) in Russian. (Thermo; Experimental)

49Wra: W.J. Wrazej, "Lattice Spacing of Retained Austenite in Iron-Carbon Alloys," *Nature*, *163*, 212-213 (1949). (Crys Structure; Experimental)

50Arb: M.P. Arbuzov, "The Structure of Martensite Electrolytically Separated from Hardened Steel," *Dokl. Akad. Nauk SSSR*, *74*, 1085-1087 (1950) in Russian; *Struct. Rep.*, *13*, 62 (1950). (Crys Structure; Experimental)

50Eck: H.C. Eckstrom and W.A. Adcock, "A New Iron Carbide in Hydrocarbon Synthesis Catalysts," *J. Am. Chem. Soc.*, *72*(2), 1042-1043 (1950). (Meta Phases; Experimental)

50Jac: K.H. Jack, "Results of Further X-Ray Structural Investigations of the Iron-Carbon and Iron-Nitrogen System and of Related Interstitial Alloys," *Acta Crystallogr.*, *3*, 392-394 (1950). (Meta Phases, Crys Structure; Experimental)

50Maz: J. Mazur, "Lattice Parameters of Martensite and Austenite," *Nature*, *166*, 828 (1950). (Crys Structure; Experimental)

50Wer: C.A. Wert, "Solid Solubility of Cementite in Alpha Iron," *Trans. AIME*, *188*, 1243-1244 (1950). (Equi Diagram, Thermo; Experimental; #)

51Bor1: G. Borelius, "Kinetics of Precipitation in Supercooled Solid Solutions," *Trans. AIME*, *191*(6), 477-484 (1951). (Equi Diagram; Experimental; #)

51Bor2: G. Borelius and S. Berglund, "Calorimetric Study of the Precipitation of Carbon Dissolved in α-Iron," *Ark. Fys.*, *4*(4), 173-182 (1951). (Equi Diagram; Experimental; #)

51Dar: L.S. Darken and R.W. Gurry, "Free Energy of Formation of Cementite and the Solubility of Cementite in Austenite," *Trans. AIME*, *191*(11), 1015-1018 (1951). (Equi Diagram; Experimental; #)

51Sch: E. Scheil, "Thermodynamics and Synthesis of Iron-Carbon Alloys," *Arch. Eisenhuttenwes.*, *22*(1-2), 37-52 (1951) in German. (Thermo; Theory; #)

52Chi: J. Chipman, R.M. Alfred, L.W. Gott, R.B. Small, D.M. Wilson, C.N. Thomson, D.L. Guermsey, and J.C. Fulton, "The Solubility of Carbon in Molten Iron and in Iron-Silicon and Iron-Manganese Alloys," *Trans. ASM*, *44*, 1215-1232 (1952). (Equi Diagram; Experimental; #)

52Fal: G. Falkanhagen and W. Hofmann, "Observation of Rapidly Quenched Iron-Carbon Melts," *Arch. Eisenhuttenwes.*, *23*(1-2), 73-74 (1952) in German. (Equi Diagram, Crys Structure; Experimental; #)

52Kit: J.A. Kitchener, J.O.M. Bockris, and D.A. Spratt, "Solutions in Liquid Iron. Part 2. The Influence of Sulphur on the Solubility and Activity Coefficient of Carbon," *Trans. Faraday Soc.*, *48*, 608-617 (1952). (Equi Diagram; Experimental; #)

53Coh: E.M. Cohn and L.J.E. Hofer, "Some Thermal Reactions of the Higher Iron Carbides," *J. Chem. Phys.*, *21*(2), 354-359 (1953). (Meta Phases, Crys Structure, Magnetism; Experimental)

53Dar: L.S. Darken and R.W. Gurry, *Physical Chemistry of Metals*, McGraw-Hill, Inc., New York, (1953). (Equi Diagram, Thermo; Theory; #)

53Hou: E. Houdremont and O. Krisement, "Study on Undercooling of Transformation Processes as the Groundwork for Martensitic Transformation," *Arch. Eisenhüttenwes.*, *24*(1-2), 53-68 (1953) in German. (Crys Structure; Experimental)

53Ric: F.D. Richardson and W.E. Dennis, "Thermodynamic Study of Dilute Solutions of Carbon in Molten Iron," *Trans. Faraday Soc.*, *49*, 171-180 (1953). (Thermo; Experimental)

53Rob: C.S. Roberts, "Effect of Carbon on the Volume Fractions and Lattice Parameters of Retained Austenite and Martensite," *J. Met.*, *5*(2), 203-204 (1953). (Crys Structure; Experimental)

53San: K. Sanbongi and M. Ohtani, "On Activities of Coexisting Elements in Molten Iron. I. The Activity of Carbon in Molten Iron," *Sci. Rep. Res. Inst. Tohoku Univ. A*, *5*, 263-270 (1953). (Thermo; Experimental)

53Wil: G.K. Williamson and R.E. Smallman, "X-Ray Evidence for the Interstitial Position of Carbon in α Iron," *Acta Crystallogr.*, *6*, 361-362 (1953). (Crys Structure; Experimental)

54Hil: M. Hillert, "Solubility of Carbon in Ferrite," *Acta Metall.*, *2*(1), 11-14 (1954). (Equi Diagram, Thermo; Theory; #)

55Hil: M. Hillert, "Solubility of Cementite in Liquid Iron," *Acta Metall.*, *3*(1), 37-38 (1955). (Equi Diagram, Thermo; Theory; #)

55Lag: G. Lagerberg and A. Josefsson, "Influence of Grain Boundaries on the Behavior of Carbon and Nitrogen in α-Iron," *Acta Metall.*, *3*(5), 236-244 (1955). (Equi Diagram; Experimental)

55Lin: E. Lindstrand, "A Method for the Measurement of Elastic Relaxation, and its Use for Determination of the Solubility of Carbon in α-Iron," *Acta Metall.*, *3*(9), 431-435 (1955). (Equi Diagram; Experimental; #)

55Mat: S. Matoba and S. Banya, "Equilibrium of Carbon and Oxygen in Molten Iron Saturated with Carbon," *Tech. Rep. Tohoku Univ.*, *20*, 131-141 (1955). (Equi Diagram; Experimental; #)

55Tur: E.T. Turkdogan and L.E. Leake, "Thermodynamics of Carbon Dissolved in Iron Alloys. Part I: Solubility of Carbon in Iron-Phosphorus, Iron-Silicon, and Iron-Manganese Melts," *J. Iron Steel Inst.*, *179*(1), 39-43 (1955). (Equi Diagram; Experimental; #)

56Nag: S. Nagakura, "Study of Iron Carbides by Electron Diffraction. II. Phase Transition of the Carbides," *Nippon Kinzoku Gakkai-shi*, *20*, 465-468 (1956) in Japanese. (Meta Phases; Experimental)

56Pin: Z.G. Pinsker and S.V. Kaverin, "Electron-Diffraction Determination of the Structure of Iron Carbide Fe_4C," *Kristallografiya*, *1*(1), 66-72 (1956) in Russian; TR: *Sov. Phys. Crystallogr.*, *1*(1), 48-53 (1956). (Meta Phases, Crys Structure; Experimental)

56Pop: N.M. Popova, "Carbide Analysis of Steel," Moscow (1956); quoted in [Elliott]. (Crys Structure; Experimental)

56Ris: A. Rist and J. Chipman, "Activity of Carbon Dissolved in Liquid Iron," *Rev. Metall., Mem.*, *53*, 796-807 (1956) in French. (Thermo; Experimental)

56Tur: E.T. Turkdogan, L.E. Leake, and C.R. Masson, "Thermodynamics of Iron-Carbon Melts," *Acta Metall.*, *4*(7), 396-406 (1956). (Equi Diagram, Thermo; Theory)

57Fru: R. Fruchart and A. Michel, "New Nickel Boride Ni_3B with the Same Structure as Cementite," *Compt. Rend.*, *245*(2), 171-172 (1957) in French. (Crys Structure; Experimental)

57Gud: N.V. Gudkova, E.I. Levina, and V.A. Tolomasov, "Investigation of the Carbide Phases of Tempered Carbon Steel," *Fiz. Met. Metalloved.*, *4*(3), 500-504 (1957) in Russian; TR: *Phys. Met. Metallogr.*, *4*(3), 91-94 (1957). (Crys Structure; Experimental)

57Pin: Z.G. Pinsker and S.V. Kaverin, "Electron Diffraction Study of Nitrides and Carbides of Transition Metals," *Kristallografiya*, *2*, 386-392 (1957) in Russian; TR: *Sov. Phys. Crystallogr.*, *2*, 380-387 (1957). (Meta Phases; Experimental)

57Vin: E.Z. Vintaikin, "The Determination of the Vapor Pressure of Iron over Austenite," *Dokl. Akad. Nauk USSR*, *117*, 632-634 (1957). (Thermo; Experimental)

58Gen: P. Gendrel and L. Jacque, "Contribution to the Study of the Iron-Carbon Equilibrium Diagram," *Compt. Rend.*, *246*(4), 596-599 (1958) in French. (Equi Diagram; Experimental; #)

58Mar: F. Marion and R. Faivre, "Stoichiometries of Cementite and Hägg Carbide," *Compt. Rend.*, *247*(14), 1118-1120 (1958) in French. (Meta Phases; Experimental)

58Pet: E.F. Petrova, M.I. Lapshina, and L.A. Shvartsman, "Solubility of Carbon in α-Iron," *Dokl. Akad. Nauk SSSR*, *121*, 1021-1024 (1958) in Russian; TR: *Sov. Phys. Dokl.*, *3*, 872-876 (1958). (Equi Diagram; Experimental; #)

58Ska: Yu.A. Skakov, U.N. Chernikova, and O.V. Sharshatkina, "The Structure and Composition of the Carbide in Low-Annealed Steel," *Dokl. Akad. Nauk SSSR*, *118*, 284-285 (1958) in Russian; TR: *Sov. Phys. Dokl.*, *3*, 151-153 (1958). (Meta Phases; Experimental)

59Fuw: T. Fuwa and J. Chipman, "Activity of Carbon in Liquid-Iron Alloys," *Trans. Metall. Soc. AIME*, *215*(8), 708-716 (1959). (Thermo; Experimental)

59Heu: T. Heumann and J. Grosse-Wordemann, "Investigation of the Stable and Metastable Equilibria of Iron-Carbon Alloys," *Arch. Eisenhüttenwes.*, *30*(1), 35-39 (1959) in German. (Equi Diagram; Experimental; #)

59Hsu: C.C. Hsu, A.Yu. Poljakov, and A.M. Samarin, *Izv. V.U.Z. Chernaya. Metall.*, (11), 3-12 (1959); quoted in [Hultgren; B]. (Thermo; Experimental)

59Nag: S. Nagamura, "Study of Metallic Carbides by Electron Diffraction. Part III. Iron Carbides," *J. Phys. Soc. Jpn.*, *14*(2), 186-195 (1959). (Meta Phases, Crys Structure; Experimental)

59Sin: J. Singer and E.S. Anolick, "Solubility of Carbon in Iron as Determined by the Magnetic Aftereffect," *J. Appl. Phys.*, *30*(4), 193S-194S (1959). (Equi Diagram; Experimental; #)

59Smi1: R.P. Smith, "The Solubility of Cementite in Austenite," *Trans. Metall. Soc. AIME*, *215*(12), 954-957 (1959). (Equi Diagram; Experimental; #)

59Smi2: R.P. Smith and L.S. Darken, "The Iron-Carbon Eutectoid Temperature," *Trans. Metall. Soc. AIME*, *215*(8), 727-728 (1959). (Equi Diagram; Experimental; #)

59Syu: T. Syu, A.V. Polyakov, and A.M. Samarin, *Izv. V.U.Z. Chernaya Metall.*, *2*(11), 3-12 (1959)

***60Buc:** R.A. Buckley and W. Hume-Rothery, "Liquidus and Solidus Relations in Iron-Rich Iron-Carbon Alloys," *J. Iron Steel Inst.*, *196*(12), 403-406 (1960). (Equi Diagram; Experimental; #)

60Joh: W.D. Johnston, R.R. Heikes, and S. Petrolo, "The Preparation of Fine Powder Hexagonal Fe_2C and Its Coercive Force," *J. Phys. Chem.*, *64*(11), 1720-1722 (1960). (Meta Phases; Experimental)

60Sch: H. Schenck and H. Kaiser, "Investigation on the Activities of Carbon in Crystalline Binary and Ternary Iron-Carbon Alloys," *Arch. Eisenhüttenwes.*, *31*(4), 227-235 (1960) in German. (Thermo; Experimental)

60Sin: J. Singer and E.S. Anolick, "The Solubility of Carbon in Alpha-Fe as Determined by the Time Decay of Permeability," *Trans. Metall. Soc. AIME*, *218*(6), 405-409 (1960). (Equi Diagram; Experimental; #)

61Ben: M.G. Benz and J.F. Elliott, "The Austenite Solidus and Revised Iron-Carbon Diagram," *Trans. Metall. Soc. AIME*, *221*(4), 323-331 (1961). (Equi Diagram, Thermo; Experimental; #)

61Sch1: E. Scheil, T. Schmidt, and J. Wunning, "Determination of Equilibrium of Carbon Monoxide-Carbon Dioxide Mixture with the γ-Solid Solution, with Cementite, and with Graphite," *Arch. Eisenhuttenwes.*, *32*(4), 251-260 (1961) in German. (Equi Diagram; Experimental; #)

61Sch2: H. Schenck and G. Perbix, "Thermodynamics of Ternary Systems Iron-Carbon-Copper, Iron-Carbon-Tin, and Iron-Carbon-Antimony. Part 1. Solubility of Graphite in the Temperature Range from 1200 to 1600 °C," *Arch. Eisenhüttenwes.*, *32*(2), 123-127 (1961) in German. (Equi Diagram, Thermo; Experimental; #)

61Stu: W. Stuckens and A. Michel, "Variations in the Stoichiometry of Pure Cementite," *Compt. Rend.*, *253*(21), 2358-2360 (1961) in French. (Crys Structure, Magnetism; Experimental)

62Buc: R.A. Buckley and W. Hume-Rothery, comment *Trans. Metall. Soc. AIME*, *224*, 625 (1962). (Equi Diagram; Theory)

62Gar: A.I. Gardin, "An Electron-Diffraction Study of the Structure of Cementite," *Kristallografiya*, *7*(6), 854-861 (1962) in Russian; TR: *Sov. Phys. Crystallogr.*, *7*(6), 694-700 (1963). (Crys Structure; Experimental)

62Mei: D. Meinhardt and O. Krisement, "Structure Investigation of Carbides of Iron, Tungsten, and Chromium with Thermal Neutrons," *Arch. Eisenhüttenwes.*, *33*(7), 493-499 (1962) in German. (Crys Structure; Experimental)

62Oke: S. Oketani and S. Nagakura, "Electron Diffraction Studies on the Crystal Structures of Carbides of Iron, Cobalt, and Nickel," *J. Phys. Soc. Jpn.*, *17*, Suppl. B-II, 235 (1962). (Crys Structure; Experimental)

62Sen: J.P. Senateur. R. Fruchart, and A. Michel, "Formula and Crystal Structure of Hägg Carbide," *Compt. Rend.*, *255*(14), 1615-1616 (1962) in French. (Meta Phases, Crys Structure; Experimental)

62Smi: R.P. Smith, "The Diffusivity and Solubility of Carbon in Alpha-Iron," *Trans. Metall. Soc. AIME*, *224*(2), 105-111 (1962). (Equi Diagram; Experimental; #)

63Ers: T.P. Ershova and E.G. Ponyatovskii, "The Effect of Pressure on the Graphite-Cementite Equilibrium in the Iron-Carbon System," *Dokl. Akad. Nauk SSSR*, *151*(6), 1364-1367 (1963) in Russian; TR: *Dokl. Chem. Proc. Acad. Sci. USSR*, *151*, 724-727 (1963). (Thermo; Theory)

63Fel: U. Feldman, "Thermodynamics of Iron-Rich and Carbon-Containing Ternary Alloys," *Arch. Eisenhüttenwes.*, *34*(1), 49-54 (1963) in German. (Crys Structure, Thermo; Experimental)

63Hil: J.E. Hillard, "Iron-Carbon Phase Diagram: Isobaric Sections of the Eutectoid Region at 35, 50, and 65 Kilobars," *Trans. Metall. Soc. AIME*, *227*(4), 429-438 (1963). (Pressure; Experimental; #)

63Loe: C. Loentaritis, "Equilibrium Investigation of Carbon Saturated Iron-Manganese-Sulfur Solutions," D. Eng. thesis, Tech. Inst. Aachen (1963) in German. (Equi Diagram; Experimental;

63Lya: B.G. Lyashchenko and L.M. Sorokin, "Determination of the Position of Carbon in Cementite by the Neutron Diffraction Method," *Kristallografiya*, *8*(3), 382-387 (1963) in Russian; TR: *Sov. Phys. Crystallogr.*, *8*(3), 300-304 (1963). (Crys Structure; Experimental; #)

63Mor: T. Mori, K. Fujimura, and H. Kanoshima, "Effects of Aluminum, Sulfur, and Vanadium on the Solubility of Graphite in Liquid Iron," *Mem. Fac. Eng., Kyoto Univ.*, *25*(1), 83-105 (1963). (Equi Diagram; Experimental)

63Sen: J.P. Senateur and R. Fruchart, "Structural Analogy between Iron Carbides Fe_3C and Fe_5C_2," *Compt. Rend.*, *256*, 3114-3117 (1963) in French. (Meta Phases, Crys Structure; Experimental)

64Bar: G.H. Barton and B. Gale, "The Structure of a Pseudo-Hexagonal Iron Carbide," *Acta Crystallogr.*, *17*, 1460-1462 (1964). (Crys Structure; Experimental)

64Bun: K. Bungardt, J. Priesendanz, and G. Lehnert, "Influence of Chromium on Carbon Activity in the System Iron-Chromium-Carbon at 1000 °C," *Arch. Eisenhüttenwes.*, *35*, 999-1007 (1964) in German. (Thermo; Experimental)

64Cah: J.A. Cahill, A.D. Kirshenbaum, and A.V. Grosse, "The Solubility of Carbon in Liquid Iron to 3160 K and Viscosity Estimates of Fe-C Solutions to 2500 K," *Trans. ASM*, *57*(2), 417-426 (1964). (Equi Diagram; Experimental; #)

64Fis: E. Fisher, "Experimental Investigation and Thermodynamic Calculation of the Liquidus Line of Iron in the System Iron-Carbon," thesis, Tech. Univ. Clausthal (1964) in German. (Equi Diagram; Experimental; #)

64Her1: F.H. Herbstein and J. Smuts, "Comparison of X-Ray and Neutron-Diffraction Refinements of the Structure of Cementite Fe_3C," *Acta Crystallogr.*, *17*, 1331-1332 (1964). (Crys Structure; Experimental)

64Her2: F.H. Herbstein and J.A. Snyman, "Identification of Eckstrom-Adcock Iron Carbide as Fe_7C_3," *Inorg. Chem.*, *3*(6), 894-896 (1964). (Meta Phases, Crys Structure; Experimental)

64Sch: E. Schurmann, T. Schmidt, and H. Wegener, *Giesserei, Tech. Beih.*, *16*, 91-98 (1964); quoted in [Hultgren; B]. (Equi Diagram, Thermo; Experimental)

64Ver: A.A. Vertman, V.K. Grigovich, N.A. Nedumov, and A.M. Samarin, "Investigation of the Hypereutectoidal Range of the Iron-Carbon System (2.88 to 27 at.% C)," *Dokl. Akad. Nauk SSSR*, *159*(1), 121-124 (1964) in Russian; TR: *Dokl. Chem. Proc. Acad. Sci. USSR*, *159*, 1131-1134 (1964). (Equi Diagram; Experimental; #)

64Yer: T.P. Yershova and Ye.G. Ponyatovskiy, "Effect of High Pressures on the Phase Equilibrium Line of the Eutectoid Part of the Iron-Carbon Diagram," *Fiz. Met. Metalloved.*, *17*(4), 584-591 (1964) in Russian; TR: *Phys. Met. Metallogr.*, *17*(4), 97-105 (1964). (Pressure, Thermo; Experimental; #)

65Hud: R.M. Hudson, A.W. Abel, and G.L. Stragand, "Equilibrium Studies for the Reaction C (in Steel) + H_2O = CO + H_2," *Trans. Metall. Soc. AIME*, *233*(5), 879-883 (1965). (Thermo; Experimental)

65Ver: A.A. Vertman, V.K. Grigovich, N.A. Nedumov, and A.M. Samarin, "The Hypereutectoidal Part of the Iron-Carbon Phase Diagram," *Liteinoe Proizvod.*, (2), 27 (1965). (Equi Diagram; Experimental; #)

66Dug: M.J. Duggin and L.J.E. Hofer, "Nature of χ-Iron Carbide," *Nature*, *212*, 248 (1966). (Crys Structure; Experimental)

66Hof: L.J.E. Hofer, "Nature of the Carbides of Iron," *U.S. Bureau Mines Bull.*, *631* (1966). (Magnetism; Experimental)

66Jac: K.H. Jack and S. Wild, "Nature of χ-Carbide and Its Possible Occurrence in Steels," *Nature*, *212*, 248-250 (1966). (Crys Structure; Experimental)

66Nak: Y. Nakagawa, K. Suzuki, and M. Fukumoto, "Equilibrium of Carbon and Oxygen in Molten Iron Saturated with Carbon," *Trans. Jpn. Inst. Met.*, *7*(1), 23-31 (1966). (Equi Diagram; Experimental; #)

67Fil: E.S. Filippov, V.K. Grigorovich, and A.M. Samarin, "Structural Transformations in Iron-Carbon Melts," *Dokl. Akad. Nauk, SSSR*, *173*(3), 564-566 (1967) in Russian. (Equi Diagram; Experimental; #)

67Orr: R.L. Orr and J. Chipman, "Thermodynamic Functions of Iron," *Trans. Metall. Soc. AIME*, *239*(5), 630-633 (1967). (Thermo; Theory)

67Sen: J.P. Senateur, "Contribution to the Study of Magnetism and Structure of Hägg Carbide," *Ann. Chem.*, *2*, 103-122 (1967) in French. (Crys Structure; Experimental)

67Swa: J.C. Swartz, "The Solubility of Cementite Precipitates in Alpha Iron," *Trans. Metall. Soc. AIME*, *239*, 68-75 (1967). (Equi Diagram; Experimental; #)

68Bur: B.P. Burylev, "Concentration Dependence of the Interaction Energy for Short-Range Order in Binary and Ternary Iron Alloys," *Zh. Fiz. Khim.*, *42*(3), 628-636 (1968) in Russian; TR: *Russ. J. Phys. Chem.*, *42*(3), 333-336 (1968). (Thermo; Theory)

68Dug: M.J. Duggin, "Thermally Induced Phase Transformations in Iron Carbides," *Trans. Metall. Soc. AIME*, *242*(6), 1091-1100 (1968). (Meta Phases, Crys Structure; Experimental)

68Fis: E. Fisher, "Contribution to Calorimetry and Thermodynamics of Iron-Carbon Alloys," D. Eng. thesis, Tech. Univ. Clausthal (1968) in German. (Thermo; Theory)

68Haw: G.L. Hawkes and D.R. Morris, "A Study of the Thermodynamics of Carbon in Austenite by an Electrochemical Method," *Trans. Metall. Soc. AIME*, *242*(6), 1083-1089 (1968). (Thermo; Experimental)

68Ino: H. Ino, T. Moriya, F.E. Fujita, Y. Maeda, Y. Ono, and Y. Inokuti, "A Study of the Mossbauer Effect During the Tempering of Iron-Carbon Martensite," *J. Phys. Soc. Jpn.*, *25*(1), 88-99 (1968). (Crys Structure; Experimental)

68Mor: T. Mori, K. Fujimura, H. Okajima, and A. Yamauchi, *Mem. Fac. Eng. Kyoto Univ.*, *30*(3) 363-372 (1968). (Thermo; Experimental)

68Poi: D.R. Poirier, "Activity of Carbon in Austenite," *Trans. Metall. Soc. AIME*, *242*(4), 685-690 (1968). (Thermo; Experimental)

68Shv: L.A. Shvartman and I.A. Tomilin, "Some Problems of the Thermodynamics of Iron-Carbon Melts," Japan-USSR Joint Symposium on Physical Chemistry of Metallurgical Processes, Moscow, 13-15 (1968). (Thermo; Theory)

68Wad: T. Wada, "Thermodynamics of the α-γ Transformation of Iron Alloys," *Trans. Iron Steel Inst. Jpn.*, *8*(1), 1-13 (1968). (Equi Diagram, Thermo; Experimental)

69Ban: S. Ban-ya, J.F. Elliott, and J. Chipman, "Activity of Carbon in Fe-C Alloys at 1150 °C," *Trans Metall. Soc. AIME*, *245*(6), 1199-1206 (1969). (Thermo; Experimental)

69Fru: R. Fruchart and A. Rouault, "On the Existence of Twins in the Orthorhombic Isomorphous Carbides Cr_7C_3, Mn_7C_3, Fe_7C_3," *Ann.*

Chim., *4*, 143-145 (1969) in French. (Meta Phases, Crys Structure; Experimental)

69Gri: V.K. Grigorovich, "The Polymorphism of Iron and the Electron Structure of Iron Alloys," *Izv. Akad. Nauk SSSR, Met.*, (1), 53-68 (1969) in Russian; TR: *Russ. Metall.*, (1), 17-29 (1969). (Equi Diagram, Pressure; Experimental; #)

69Kra: G. Kraume, "Investigation on the Influence of Alloying Elements Si, P, Ni, and Mn on the Form of the Liquidus Line of Iron Corresponding to Ternary and Higher-Order Liquids Fe-C-X," thesis, Tech. Univ. Clausthal (1969) in German. (Equi Diagram; Experimental; #)

69Ruh: R.C. Ruhl and M. Cohen, "Splat Quenching of Iron-Carbon Alloys," *Trans. Metall. Soc. AIME*, *245*(2), 241-251 (1969). (Meta Phases, Crys Structure; Experimental)

69Swa: J.C. Swartz, "The Solubility of Graphite and Cementite in (Alpha, Delta) Iron," *Trans. Metall. Soc. AIME*, *245*(5), 1083-1092 (1969). (Equi Diagram; Experimental; #)

70Ban: S. Ban-ya, J.F. Elliott, and J. Chipman, "Thermodynamics of Austenitic Fe-C Alloys," *Metall. Trans.*, *1*(5), 1313-1320 (1970). (Equi Diagram, Thermo; Experimental; #)

70Chi: J. Chipman, "Thermodynamics of Liquid Fe-C Solutions," *Metall. Trans.*, *1*(8), 2163-2168 (1970). (Thermo; Experimental)

70Rid: N. Ridley and H. Stuart, "Partial Molar Volumes from High-Temperature Lattice Parameters of Iron-Carbon Austenites," *Met. Sci. J.*, *4*(6) 219-222 (1970). (Crys Structure; Experimental)

70Ver: L.F. Vereshchagin, L.E. Shterenberg, and V.N. Slesarev, "The Role of Fe_3C Carbide in the Synthesis of Diamond," *Dokl. Akad. Nauk SSSR*, *192*(4), 768-770 (1970) in Russian; TR: *Sov. Phys. Dokl.*, *15*(6), 556-558 (1970). (Pressure; Experimental; #)

71Gac: J.-C. Gachon and B. Schmitt, "Determination by X-ray of the Coefficients of Thermal Expansion of Cementite in the [100], [010], and [001] Directions," *C.R. Acad. Sci. Paris*, *272*(1), 428-431 (1971).

71Har: H. Harvig, "Iron-Carbon System in the Temperature Range 500-1150°," *Jernkont. Ann.*, *155*(4), 157-161 (1971). (Equi Diagram, Thermo; Theory)

71Wad: T. Wada, H. Wada, J.F. Elliott, and J. Chipman, "Thermodynamics of the Fcc Fe-Ni-C and Ni-C Alloys," *Metall. Trans. A*, *2*(8), 2199 (1971). (Equi Diagram; Experimental)

***72Chi:** J. Chipman, "Thermodynamics and Phase Diagram of the Fe-C System," *Metall. Trans.*, *3*(1), 55-64 (1972). (Equi Diagram, Thermo; Theory; #)

72Hir: Y. Hirotsu and S. Nagakura, "Crystal Structure and Morphology of the Carbide Precipitated from Martensitic High Carbon Steel During the First Stage of Tempering," *Acta Metall.*, *20*(4), 645-655 (1972). (Meta Phases, Crys Structure; Experimental)

72Yav: V.I. Yavoyskiy, A.G. Svyazhin, A.F. Vishkarev, K.P. Nguen, D.A. Romanovich, and G.M. Chursin, *Izv. Akad. Nauk, SSSR, Met.*, (3), 33-40 (1972) in Russian; TR: *Russ. Metall.*, (3) 24-30 (1972). (Thermo; Experimental)

73Zhu1: A.A. Zhukov, L.E. Shterenberg, V.D. Kal'ner, V.A. Shalashov, N.A. Berezovskaya, V.K. Thomas, and R.L. Snezhnoi, "Phase Diagram of the Iron-Diamond System," *Dokl. Akad. Nauk SSSR*, *211*(1), 145-157 (1973) in Russian; TR: *Sov. Phys. Chem.*, *24*, 548-550 (1973). (Pressure; Experimental; #)

73Zhu2: A.A. Zhukov, L.E. Shterenberg, V.A. Shalashov, V.K. Thomas, and N.A. Berezovskaya, "The Iron-Carbon System. New Developments—I. The Pseudohexagonal Iron Carbide Fe_7C_3 and the Fe_3C-Fe_7C_3 Eutectic," *Acta Metall.*, *21*(3), 195-197 (1973). (Pressure; Experimental)

73Zhu3: A.A. Zhukov, L.E. Shterenberg, V.A. Shalashov, V.K. Thomas, and N.A. Berezovskaya, "The Pseudohexagonal Iron Carbide Fe_7C_3 and the Fe_3C-Fe_7C_3 Eutectic in the Fe-C System," *Izv. Akad. Nauk SSSR, Met.*, (1), 181-184 (1973) in Russian; TR: *Russ. Metall.*, (1), 127-130 (1973). (Pressure; Experimental)

74Bas: M.I. Baskes, "Phase Stability of Iron Base Alloys," *Mater. Sci. Eng.*, *15*, 195-202 (1974). (Equi Diagram, Thermo; Theory; #)

76Kur: G.V. Kurdjumov, "Martensite Crystal Lattice, Mechanism of Austenite-Martensite Transformation and Behavior of Carbon Atoms in Martensite," *Metall. Trans. A*, *7*(7), 999-1011 (1976). (Crys Structure; Experimental)

78Sch: I. Schmidt and E. Hornbogen, "The Formation of Metastable Crystalline Phases and Glasses in Splat-Cooled Fe-C Alloys," *Z. Metallkd.*, *69*(4), 221-227 (1978). (Equi Diagram, Meta Phases; Theory)

79Agr: J. Agren, "A Thermodynamic Analysis of the Fe-C and Fe-N Phase Diagram," *Metall. Trans. A*, *10*(12), 1847-1852 (1979). (Equi Diagram, Thermo; Theory; #)

***79Sch1:** E. Schurmann and R. Schmid, "A Short-Range Order Model for the Calculation of Thermodynamic Mixing Variables and Its Applications to the System Iron-Carbon," *Arch. Eisenhüttenwes.*, *50*(3), 101-106 (1979) in German. (Equi Diagram, Thermo; Theory; #)

79Sch2: E. Schurmann and R. Schmid, "The Phase Lines of the System Iron-Carbon of the Stable and Unstable Phase Equilibria of Austenite and Ferrite with Graphite and Cementite and Also the Melt," *Arch. Eisenhüttenwes.*, *50*(5), 185-188 (1979) in German. (Equi Diagram, Meta Phases, Thermo; Theory; #)

79Wil: D.L. Williamson, K. Nakazawa, and G. Krauss, "A Study of the Early Stages of Tempering in an Fe-1.2 Pct Alloy," *Metall. Trans. A*, *10*(9), 1351-1363 (1979). (Meta Phases; Experimental)

81Tan: Y. Tanaka and K. Shimizu, "Carbide Formation upon Tempering at Low Temperatures in Fe-Mn-C Alloys," *Trans. Jpn. Inst. Met.*, *22*(11), 779-788 (1981). (Meta Phases, Crys Structure; Experimental)

81Tre: C.P.O. Treutler, G. Dienel, and K. Hohmuth, "Formation of Chemical Compounds and Structural Changes Caused by the Ion Implantation of Boron and Carbon in α-Fe Films," *Thin Solid Films*, *79*(3), 201-205 (1981). (Meta Phases; Experimental)

82Chi: B. Chicco and W.R. Thorpe, "Experimental Determination of the Austenite Liquid Phase Boundaries of the Fe-C System," *Metall. Trans. A*, *13*(7), 1293-1297 (1982). (Equi Diagram; Experimental; #)

82Dra: V.M. Drako and G.A. Gumanskij, "Structural Changes in Iron after Nitrogen and Carbon Ion Implantation," *Radiat. Eff.*, *66*, 101-108 (1982). (Meta Phases; Experimental)

82Kub: O. Kubaschewski, *Iron—Binary Phase Diagrams*, Springer-Verlag, New York, 23-26 (1982). (Equi Diagram; Review; #)

82Swa: L.J. Swartzendruber, "The Iron System," *Bull. Alloy Phase Diagrams*, *3*(2), 161-165 (1982). (Equi Diagram, Crys Structure, Magnetism; Review)

83Chi: B. Chicco and W.R. Thorpe, "A Further Determination of the Austenite Solidus of the Fe-C System," *Metall. Trans. A*, *14*(2), 312-314 (1983). (Equi Diagram; Experimental; #)

83Kap: R. Kaplow, M. Ron, and N. DeCristofaro, "Mössbauer Effect Studies of Tempered Martensite," *Metall. Trans. A*, *15*(6), 1135-1145 (1983). (Meta Phases, Crys Structure; Experimental)

83Nag: S. Nagakura, Y. Hirotsu, M. Kusunoki, T. Suzuki, and Y. Nakamura, "Crystallographic Study of the Tempering of Martensitic Carbon Steel by Electron Microscopy and Diffraction," *Metall. Trans. A*, *14*(6), 1025-1031 (1983). (Crys Structure; Experimental)

***84Oht:** H. Ohtani, M. Hasebe, and T. Nishizawa, "Calculation of Fe-C, Co-C, and Ni-C Phase Diagrams," *Trans. Iron Steel Inst. Jpn.*, *24*, 857-864 (1984). (Equi Diagram, Meta Phases, Thermo; Theory; #)

85Gus: P. Gustafson, "A Thermodynamic Evaluation of the Fe-C System," *Scan. J. Metall.*, *14*, 259-267 (1985). (Equi Diagram; Thermo; Theory; #)

***85Has:** M. Hasebe, H. Ohtani, and T. Nishizawa, "Effect of Magnetic Transition on Solubility of Carbon in bcc Fe and fcc Co-Ni Alloys," *Metall. Trans. A*, *16*(5), 913-921 (1985). (Equi Diagram; Experimental; #)

85Tak: M. Takahashi, K. Nushiro, and S. Ishio, "Formation of the F.C.C. Phases in Fe-C Alloys by Rapid Quenching," *Phys. Status Solidi (a)*, *89*, K27-K29 (1985). (Meta Phases, Crys Structure; Experimental)

86Ban: O.A. Bannykh and M.E. Drits, "Iron-Carbon," *Phase Diagrams of Binary and Multi Component Systems Based on Iron. Reference Book*, Metallurgiya, Moscow, 95-100 (1986) in Russian. (Equi Diagram; Review; #)
89Oli: L.S. deOliveira, M.T.X. Silva, and J.A.H. daJornada, "Temperature and Pressure Effects on the Iron Carbides Formed by Carbon Ion Implantation," *J. Phys. Chem. Solids*, *50*(8), 763-767 (1989). (Meta Phases; Experimental)

*Indicates key paper.
#Indicates presence of a phase diagram.

C-Fe evaluation contributed by **H. Okamoto**, ASM International, Materials Park, OH 44073. This work was supported by ASM International. Literature searched through 1989. Dr. Okamoto is the Alloy Phase Diagram Program Category Editor for miscellaneous binary alloys.

The Ir-Ru (Iridium-Ruthenium) System

By H. Okamoto
ASM International

Equilibrium Diagram

The assessed Ir-Ru phase diagram (Fig. 1) was proposed by [88Ere], based on thermal, X-ray, and metallographic investigations. [64Rau] (preliminary results given in [59Rau]) also determined the (Ir) and (Ru) solvus boundaries of the Ir-Ru phase diagram, based on X-ray and metallographic investigations. [88Ere] and [64Rau] are in good agreement, except for a single point given by [64Rau] at 1900 °C and 46 at.% Ru (Fig. 1). The equi-

Table 1 Ir-Ru Crystal Structure Data

Phase	Composition, at.% Ru	Pearson symbol	Space group	Strukturbericht designation	Prototype
(Ir)	0 to 45	*cF*4	*Fm*$\bar{3}$*m*	*A*1	Cu
(Ru)	51 to 100	*hP*2	*P*6$_3$/*mmc*	*A*3	Mg

From [King1].

Table 2 Ir-Ru Lattice Parameter Data

Phase	Composition, at.% Ru	Lattice parameters, nm: a	c	Reference
(Ir)	0	0.38391	...	[King1]
	13	0.3833	...	[64Rau]
	25.1	0.3828	...	[64Rau]
	30	0.3825	...	[64Rau]
	35	0.3822	...	[64Rau]
	37.5	0.3822	...	[64Rau]
	40	0.3821	...	[64Rau]
	43	0.3818	...	[64Rau]
(Ru)	56	0.2718	0.4322	[64Rau]
	70	0.2715	0.4317	[64Rau]
	74	0.2713	0.4312	[64Rau]
	85	0.2712	0.4301	[64Rau]
	91.5	0.2708	0.4293	[64Rau]
	100	0.27053	0.42814	[King1]

Note: Data of [64Rau] were shown with a figure in [59Rau].